

Investigation of Hydraulic Fracture Water Injection in Wolfcamp Formation

By

Yousef Saeed © 2019

B.Sc., Marietta College 2017

Submitted to the graduate degree program in Chemical & Petroleum Engineering Department and the Graduate Faculty of the University of Kansas in partial fulfillment of the requirements for the degree of Master of Science.

Chair: Dr. Reza Barati

Dr. Shapour Vossoughi

Dr. Jyun-Syung Tsau

Date Defended: August 30th, 2019

The thesis committee for University of Kansas certifies that this is
the approved version of the following thesis:

Investigation of Hydraulic Fracture Water Injection in Wolfcamp Formation

Chair: Dr. Reza Barati

Date Approved:

Abstract

Hydraulic fracturing in low permeability formations is one of the most important steps in oil and gas production. A successful hydraulic fracturing will most likely result in successful oil and gas production. Designing an optimum fracture half-length will result in injecting the perfect amount of fracturing fluid which will result in better hydrocarbon production. Otherwise, injecting less fluid will result in less hydrocarbon production and injecting more fluid will result in water blockage which will reduce relative permeability and also cause phase trapping where oil and gas are trapped and will not be produced. This thesis focuses on fracture half-length and the effect of water volumes injected to generate such a length. Many models were created to test different parameters such as the effect of permeability, water saturation, and capillary pressure on the water blockage issue in Wolfcamp formation. Economic analysis was done later to show which model is the most beneficial.

Three different fracture half-length of 100ft, 200ft, and 350ft were selected for the models. Each model was tested separately with different permeability to show the effect of fracture permeability on oil and gas production. The fracture permeability, 0.1,1,10, and 100md, was used in three models, respectively.

Representative cases were selected based on the sensitivity analysis results on fractures with different fracture half-length next. Fracture permeability was changed in each model and was 5md for the first model, 10md, and 20md for the second and third model, respectively. The effect of water saturation was studied by changing the water saturation from 45% to 55% in an increment of 5% in each model. Capillary pressure was then added to test its effect on the 3 models. All models had the same capillary pressure.

Economic analysis was made to see which model is more beneficial. As fracture permeability increases the trend show an increase in hydrocarbon production. Water saturation was the conclusive parameter. Hydrocarbon production was the lowest in the first model. The first model, which has fracture half-length of 100ft, had the lowest fracture half-length, therefore less water was injected. As a result, water saturation was the lowest in this model. The second model, which has fracture half-length of 200ft, had the optimum fracture half-length which means this model had the perfect amount of injected water. Hydrocarbon production was the highest in this model. Water saturation and fracture permeability were higher in this model than the previous one. The last model, which has fracture half-length of 350ft, had the highest fracture half-length. This model had the highest amount of injected water. Injecting more water than needed resulted in formation damage. Water was blocking the fractures and caused decrease in relative permeability. Oil and gas were trapped in the formation as a result. This model's hydrocarbon production was higher than the first model and lower than the second model. This model had the highest water saturation and fracture permeability.

Acknowledgments

I would like to thank my advisor, Dr. Barati for his effort and time to show me the correct path in this thesis. I would also like to thank the committee members: Dr. Vossoughi and Dr. Tsau for their guidance in this research.

I also wish to thank my family and friends for their unconditional support in all my endeavors.

I would like to acknowledge IHS Harmony and CMG for providing their license and applications that were helpful in this research.

Table of Contents

Introduction	1
Literature review	2
Wolfcamp formation	2
Wolfcamp Geology	4
Water management	6
Water production and water use for hydraulic fracturing	6
Produced water from conventional vs. unconventional reservoirs	6
Water sourcing in Permian basin	7
Effect of fracture volume on unconventional wells' performance	8
Formation damage caused by injected water in Wolfcamp.	9
Methodology	10
Decline curve analysis	10
CMG model	15
SCAL	17
Permeability effect	19
Water saturation effect	20
Optimum fracture half-length	21
Capillary pressure effect	21
Economic Analysis	22
Results and discussion	25
DCA – Decline curve analysis	25
First segment graphs	25

CMG models	28
Effect of fracture permeability	28
Effect of water saturation	39
Effect of Invaded water volume and Fracture Length on Production	42
Water saturation maps	47
Optimum fracture half-length	58
Effect of Capillary pressure	60
Economic analysis	64
Gas Production nowadays in Permian basin	67
Cost estimate for new model	69
Conclusions	70
Nomenclature	71
Figures	73
Second segment graphs:	73
Third segment graphs	75
4 th segment graphs	77
5 th segment graphs	79
References	82

List of Figures

Figure 1 (U.S. Energy Information Administration, 2018)	3
Figure 2 (U.S. Energy Information Administration, 2018)	4
Figure 3 Wolfcamp production map (Gaswirth, 2017).....	5
Figure 4 Water production vs use in Permian basin (B3 Data Insight Outcomes, 2019)	6
Figure 5 (Scanlon, Reedy, Male, & Walsh, 2017).....	7
Figure 6 production rate vs time (a) and cumulative gas production vs time (b) with different number of fractures. The difference is more noticeable at the early stage of production. This figure was reprinted with permission from (Gou, Song, Wu, & Killough, 2017). Copy rights are reserved ELSEVIER B.V. 2017.....	9
Figure 7 IHS Harmony, production data matching for well 23	11
Figure 8 Oil-water relative permeability curve.....	17
Figure 9 gas-oil relative permeability vs liquid saturation curve	18
Figure 10 Water saturation vs Capillary pressure.....	22
Figure 11 Injected water volume in Gal vs Q_i	26
Figure 12 Injected water volume in Gal vs D_i	26
Figure 13 Injected water volume in Gal vs b	27
Figure 14 Injected water volume in Gal vs time in months	27
Figure 15 Cumulative oil production for the first model, comparing different fracture permeability.	29
Figure 16 Cumulative gas production for the first model comparing different fracture permeability	30

Figure 17 Cumulative water production for the first model comparing different fracture permeability	31
Figure 18 Cumulative oil production for the second model comparing different fracture permeability	32
Figure 19 Cumulative gas production for the second model comparing different fracture permeability	33
Figure 20 Cumulative water production for the second model comparing different fracture permeability	34
Figure 21 Cumulative oil production for the third model comparing different fracture permeability	36
Figure 22 Cumulative gas production for the third model comparing different fracture permeability	37
Figure 23 Cumulative water production for the third model comparing different fracture permeability	38
Figure 24 Oil and gas production for the first model. $X_f = 200\text{ft}$, $k = 10\text{md}$, $S_w = 45\%$	40
Figure 25 oil gas and water production for the second model. $X_f = 200\text{ft}$, $k = 10\text{md}$, $S_w = 50\%$. Water production was included in this graph because it was selected as a representative gas for further tests.....	41
Figure 26 Oil and gas production for the third model were $X_f = 200\text{ft}$, $k = 10\text{md}$, and $S_w = 55\%$	42
Figure 27 Cumulative oil production for the 3 representative models comparing different water saturation.....	43

Figure 28 Cumulative gas production for the 3 representative models comparing different water saturation	44
Figure 29 Cumulative water production for the 3 representative models comparing different water saturation	45
Figure 30 matrix water saturation map for the last time step for the first model with no capillary pressure	47
Figure 31 fracture water saturation map for the last time step for the first model with no capillary pressure	48
Figure 32 matrix water saturation map for the last time step for the second model with no capillary pressure	49
Figure 33 fracture water saturation map for the last time step for the second model with no capillary pressure	50
Figure 34 matrix water saturation map for the last time step for the third model with no capillary pressure	51
Figure 35 fracture water saturation map for the last time step for the third model with no capillary pressure	52
Figure 36 matrix water saturation map for the last time step for the first model with capillary pressure	53
Figure 37 fracture water saturation map for the last time step for the first model with capillary pressure	54
Figure 38 matrix water saturation map for the last time step for the second model with capillary pressure	55

Figure 39 fracture water saturation map for the last time step for the second model with capillary pressure	56
Figure 40 matrix water saturation map for the last time step for the third model with capillary pressure	57
Figure 41 fracture water saturation map for the last time step for the third model with capillary pressure	58
Figure 42 Oil and gas production for model with $X_f = 250\text{ft}$, $k = 10\text{md}$, and $S_w = 51.5\%$	59
Figure 43 Cumulative oil production for the 3 representative models with capillary pressure	60
Figure 44 Cumulative gas production for the 3 representative models with capillary pressure ...	61
Figure 45 Cumulative water production for the 3 representative models with capillary pressure	62
Figure 46 Injected water volume in Gallon vs Q_i	73
Figure 47 Injected water volume in Gallon vs D_i	74
Figure 48 Injected water volume in Gallon vs b	74
Figure 49 Injected water volume in Gallon vs time in months	75
Figure 50 Injected water volume in Gallon vs Q_i	75
Figure 51 Injected water volume in Gallon vs D_i	76
Figure 52 Injected water volume in Gallon vs b	76
Figure 53 Injected water volume in Gallon vs time in months	77
Figure 54 Injected water volume in Gallon vs Q_i	77
Figure 55 Injected water volume in Gallon vs D_i	78
Figure 56 Injected water volume in Gallon vs b	78
Figure 57 Injected water volume in Gallon vs time in months	79
Figure 58 Injected water volume in Gallon vs Q_i	79

Figure 59 Injected water volume in Gallon vs Di	80
Figure 60 Injected water volume in Gallon vs b	80
Figure 61 Injected water volume in Gallon vs time in months	81

List of Tables

Table 1 PVT data	15
Table 2	19
Table 3 Models' fracture half-length and permeability	20
Table 4 Models properties	21
Table 5 Water saturation vs Capillary pressure	21
Table 6 oil, gas, and water production for the first model	31
Table 7 Oil, gas, and water production for the second model	35
Table 8 Oil, water and gas production table for the third model	38
Table 9 Effect of water saturation.....	42
Table 10 oil, gas, and water cumulative production for representative models	46
Table 11 Comparison between 3 representative models with and without capillary pressure	63
Table 12 First model economic analysis.....	64
Table 13 Second model economic analysis	65
Table 14 Third model economic analysis	65
Table 15 PV table.....	66
Table 16 NPV and IRR	66
Table 17 Expenses table.....	67
Table 18 Revenues table	68
Table 19 NPV and IRR for case where gas price is -\$0.5	68
Table 20 Expenses	69
Table 21 Net income if gas cost -\$0.5 in Permian basin	70

Introduction

Hydraulic fracturing is the most important step in oil and gas production. A successful hydraulic fracturing will come up with the best oil and gas production. Designing an optimum fracture half-length will result in injecting the perfect amount of fracturing fluid which will result in better hydrocarbon production. Otherwise, injecting less fluid will result in less hydrocarbon production and injecting more fluid will result in water blockage which will reduce relative permeability and also cause phase trapping where oil and gas are trapped and will not be produced. Fracture half-length plays a crucial role in controlling the amount of injected water. Having optimum fracture half-length means having the optimum amount of water injected which will lead to a better oil and gas recovery. We need to understand the correlation between fracture half-length (and the amount of water injected as a result of the hydraulic fracturing) and oil and gas production. One should understand whether injecting more water through larger fracture half-length will always result in a better recovery or not. Not only that, but also, we must understand the importance of injected water on the efficiency of fractures in the well.

Hydraulic fracturing and water injection is an essential step that will play a crucial role in oil and gas production. However, this process could consume hundred thousand and sometimes millions of gallons of water. Petroleum engineers know that the amount of water to be injected is not little, and fresh water injection is controversial topic not only for them, but also to the public.

Up to December of 2016, Wolfcamp formation has produced more than 962 million barrels of oil and 4.2 Tcf of gas (Gupta, Rai, Sondergeld, & Devegowda, 2017). It is one of the most productive formations in the Permian basin. The location of the Wolfcamp formation is in the Permian basin in Texas and New Mexico and its rock type is late Cretaceous shale (Gupta, Rai,

Sondergeld, & Devegowda, 2017). Wolfcamp formation's depth vary between 5,500 to 11,000ft (Pioneer Natural Resources Company, 2014).

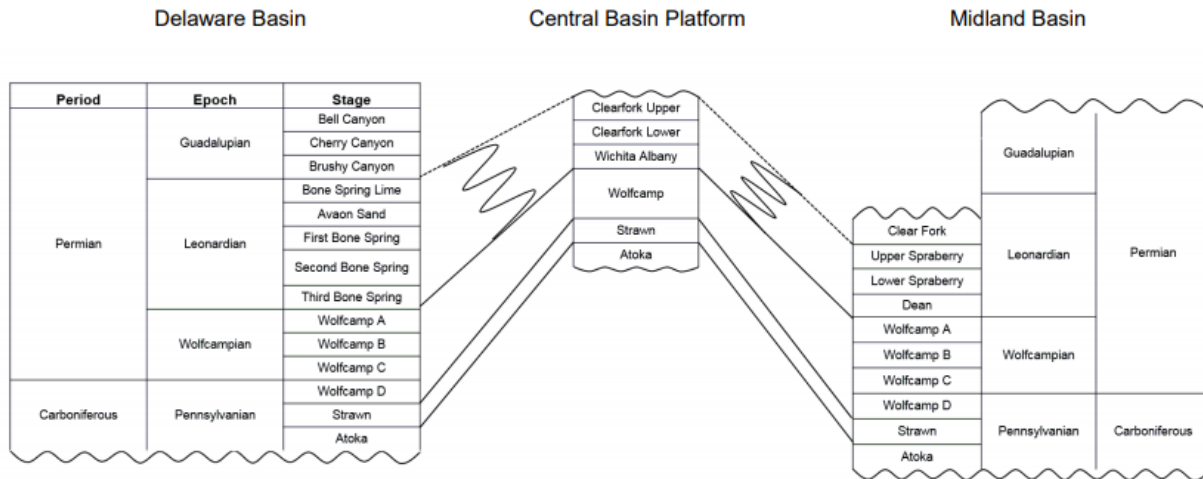
This work will discuss the correlation between hydraulic fracturing water injection and oil & gas production. This work will also discuss the effect of water injected through hydraulic fracturing on the formation and will show different models that will demonstrate the relationship between water injected through hydraulic fracturing and oil and gas production. A full economic analysis is conducted at the end.

Literature review

The Permian basin of Southeast New Mexico and West Texas has been producing hydrocarbon for around 100 years where it provided the nation with more than 33.4 billion barrels of oil and around 118 trillion cubic feet of natural gas up to September 2018 (Popova, 2018). Since 2010, more than 2000 horizontal wells were drilled only on University Land in Midland basin (Zhu, Forrest, Xiong, & Pradhan, 2018) which is one of the sub-basins that falls under the Permian basin. The Permian basin is basically consisting of many sub-basins including Delaware basin and Midland basin and it's approximately 300 miles long and 250 miles wide (Chevron, n.d.). There are more than 7,000 fields in the Permian basin across 61 counties. They all range in depth from few hundred feet up to five miles (Railroad Commision of Texas, 2019). Wolfcamp is one of the formations that is located in both Delaware and Midland basin.

Wolfcamp formation

Wolfcamp formation is between 299 – 280 million years old (Stratigraphy, n.d.). It is located in the Permian basin, specifically in Midland, Delaware, and Central basin platform. It is divided into 4 formations; Wolfcamp A, B, C, and D (U.S. Energy Information Administration, 2018).



Source: U.S. Energy Information Administration based on DrillingInfo Inc., U.S. Geological Survey.

Figure 1 (U.S. Energy Information Administration, 2018)

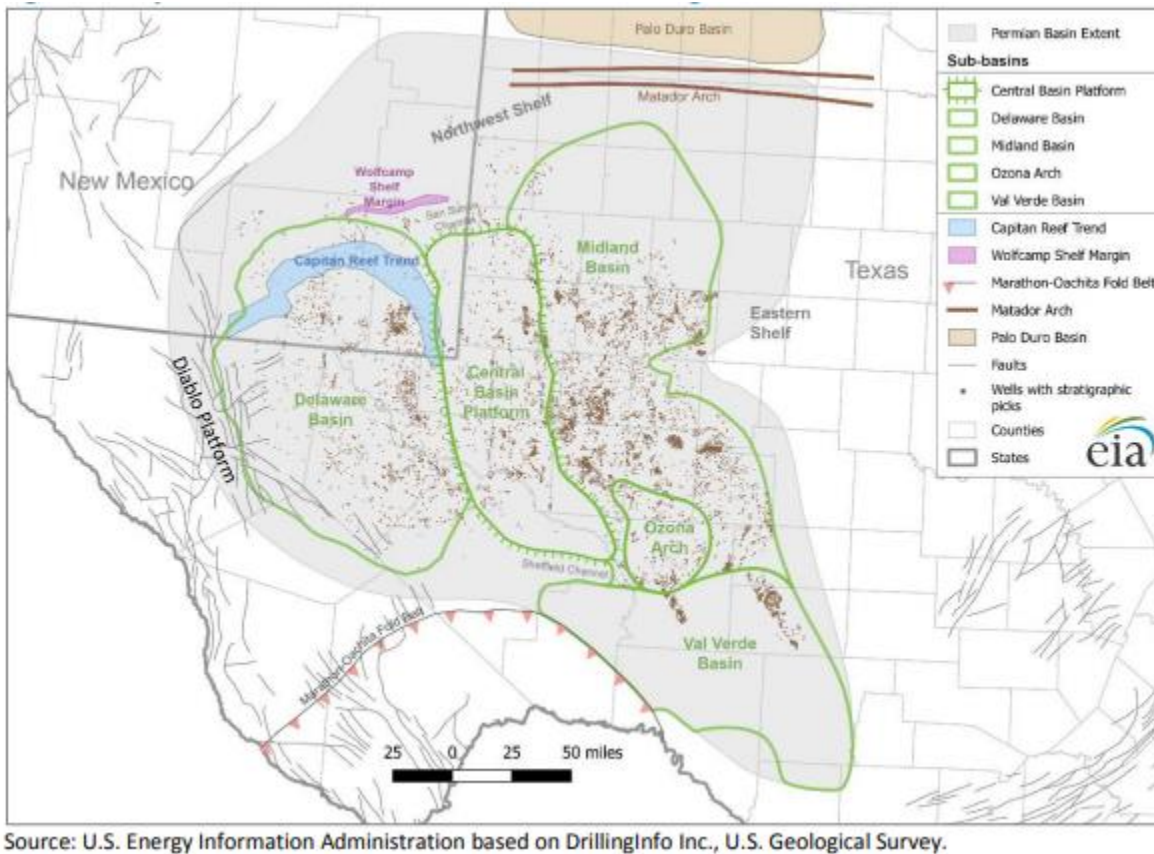


Figure 2 (U.S. Energy Information Administration, 2018)

Wolfcamp Geology

The location of Wolfcamp formation is mainly in the Permian basin between Texas and New Mexico. It is basically late Cretaceous shale (Gupta, Rai, Sondergeld, & Devegowd, Rock Typing in Wolfcamp Formation, 2017). Wolfcamp depth range from 5,500 up to 11,000ft and its thickness vary from 1,500 to 2,600ft (Securities and Exchange Commission, 2014). It is 20 – 50% Quartz, 10 – 60% Carbonate, and 10 – 45% Clay. Its porosity ranges from 2 up to 10% and its total organic compound is between 2 – 6%. The pressure gradient is between 0.55 and 0.70 psi/ft (Securities and Exchange Commission, 2014).

According to the United States geological survey, the Wolfcamp formation has produced 1.3 billion barrels of oil as of November 2016. The majority of this production comes from Midland basin where it produced 442 million barrels of oil. The undiscovered, technically recoverable resources, amount in Midland basin is 20 BBO, 16 trillion cubic feet of gas, and 1.6 billion barrels of natural gas liquid (Gaswirth, 2017). Figure 2 will show a map of oil and gas wells in Wolfcamp formation.

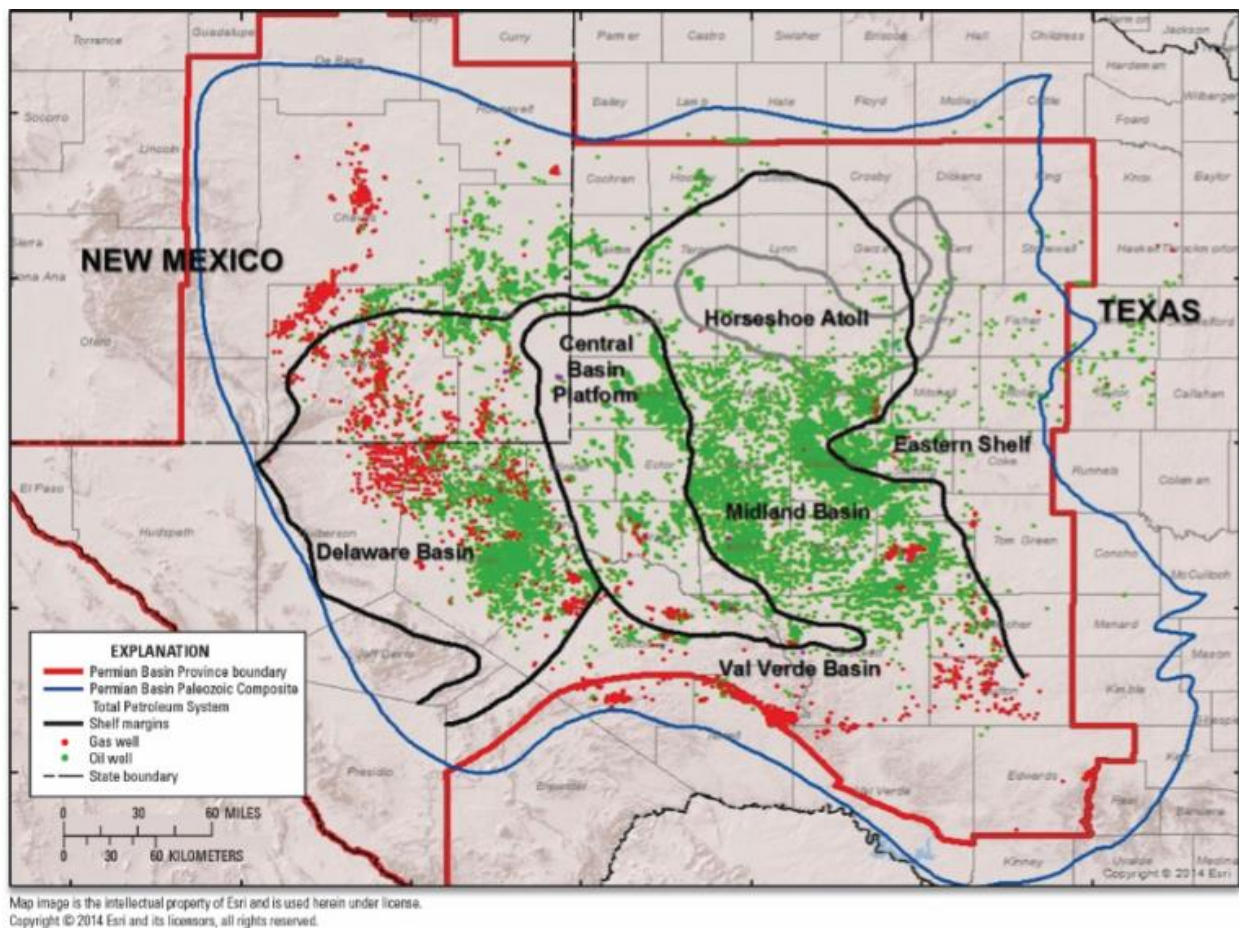


Figure 3 Wolfcamp production map (Gaswirth, 2017).

Water management

Water production and water use for hydraulic fracturing

A forecast for water production and water use in the Permian basin was published in Groundwater protection Council website. The study shows that depending on oil price, water production could increase up to 7 Bbbls per year of water in 2028.

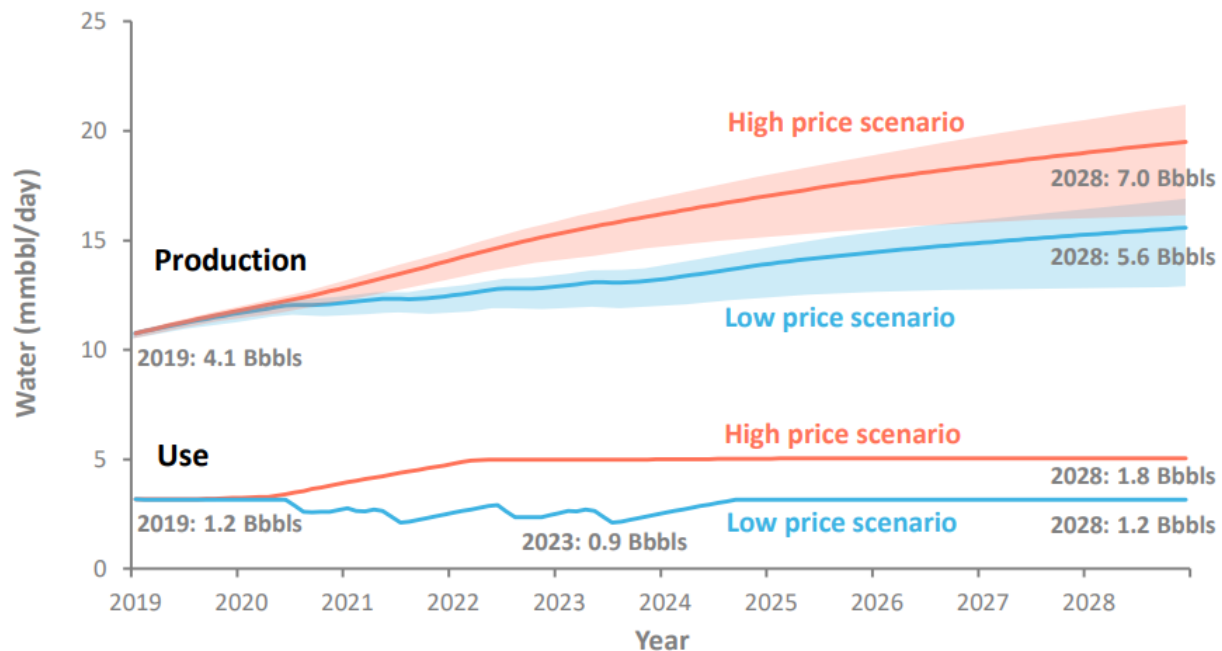


Figure 4 Water production vs use in Permian basin (B3 Data Insight Outcomes, 2019)

The same study states that in case of the high oil price, around 750 wells will be drilled each month, which is 50% more in case oil price was low (B3 Data Insight Outcomes, 2019). That demonstrate the gap in water production between the high and low-price scenario.

Produced water from conventional vs. unconventional reservoirs

Produced water amount in conventional reservoirs are much more than unconventional reservoirs. Usually, a conventional reservoir requires more water to be injected for EOR

purposes. Even though oil and gas production in conventional reservoirs in the Permian basin are 4 times more than unconventional reservoirs, it produced water could be 20 times more (Scanlon, Reedy, Male, & Walsh, 2017). Based on a study that was published in American Chemical Society, the amount of water used for injection/disposal in conventional reservoirs are more than double the amount used for unconventional. Figure 4 will show a comparison between conventional reservoirs, unconventional vertical wells, and unconventional horizontal wells in oil and gas production as well as amount of injected and produced water. Water production in conventional reservoirs are much higher in unconventional reservoirs.

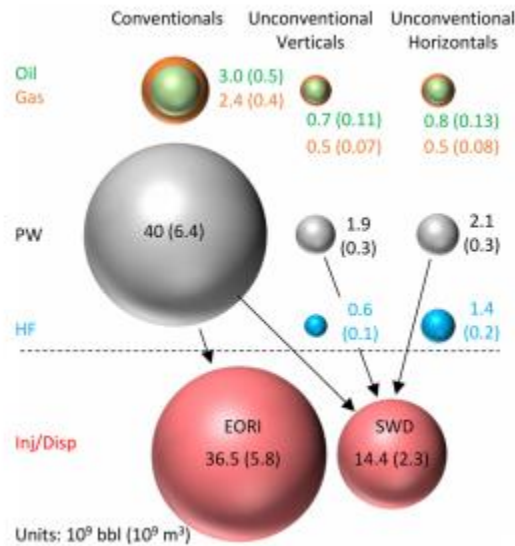


Figure 5 (Scanlon, Reedy, Male, & Walsh, 2017)

Water sourcing in Permian basin

According to Gabriel Collins, the Permian basin uses water daily roughly as much as what the city of San Antonio uses, or roughly 17 times the average daily water consumption of the city of Midland (Collins, 2018). The same study provided names of 9 companies that proclaim the reuse of produced water in the Permian basin. Apache and Devon for example, mentioned that by the

end of 2018 both companies will recycle 80% of produced water. Apache mentioned that they will use their recycled water for their fracture jobs. Cimarex is another water recycling company; they mentioned that they recycle 46% of produced water in some areas in the Wolfcamp formation and could reach up to 87% in different places in the same formation (Collins, 2018). The American Oil and Gas Reporter website mentioned another source of water in the Permian basin area which is deep freshwater aquifers (Gay & Fletcher, 2014). This option is a valid and more expensive option than water reuse. Another study supported what was found on American Oil & Gas Reporter website and mentioned that generally fresh water used for fracking jobs, is sourced (depending on availability) from groundwater or surface water (Nicot & Scanlon, 2012).

Effect of fracture volume on unconventional wells' performance

Horizontal wells with multiple hydraulic fractures are a common way to produce hydrocarbons from wells with very low permeability. Hydraulic fractures create several high conductivity flow paths that will make flow of oil and gas much easier (Zhao, Zhang, Luo, & Zhang, 2014). It will also connect existing micro-seismic natural fracture to create larger fracture network (Clarkson C. , 2013).

Higher number of fractures will also reduce fracture spacing. This will allow the well to produce more hydrocarbon as the number of fracture increases. As the number of fractures increases the production rate increases. A study conducted by (Gou, Song, Wu, & Killough, 2017) showed different number of fractures along with their production rate and cumulative gas production. As number of fractures increased, gas production increased in the early stage of production. Four different models were created, the first model had 6 fractures and the fracture spacing was 38m. the second model had 9 fractures and the fracture spacing was 25m. this is to show that as we

have more fracture numbers, fracture spacing decrease. The third and the fourth model had 12 and 15 fractures, respectively. Production rate and cumulative production were the highest in the model with the highest number of fracture and they were the lowest in the model with the lowest number of fractures.

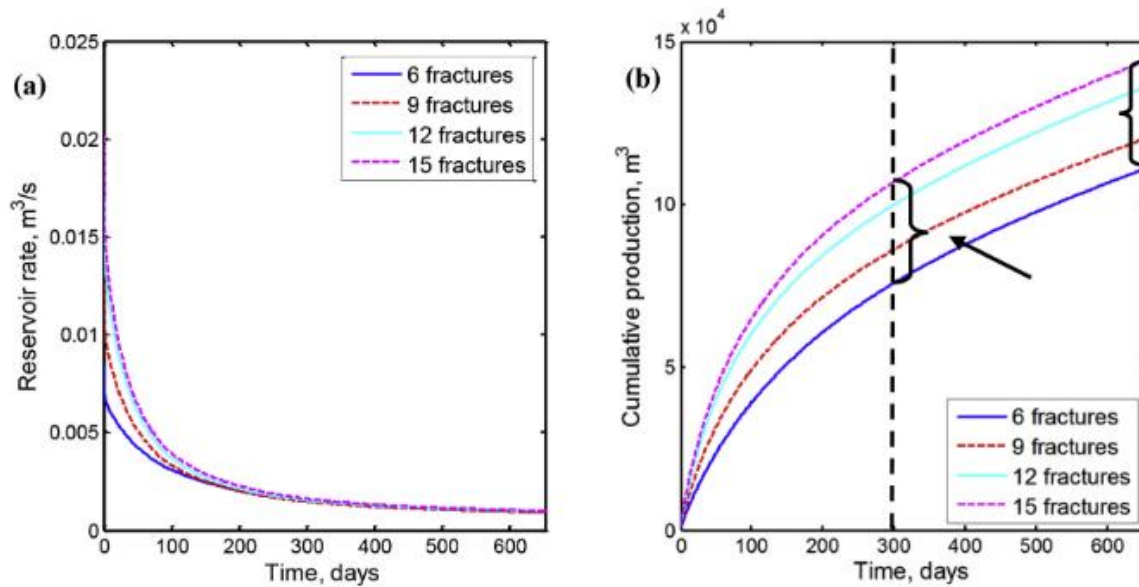


Figure 6 production rate vs time (a) and cumulative gas production vs time (b) with different number of fractures. The difference is more noticeable at the early stage of production. This figure was reprinted with permission from (Gou, Song, Wu, & Killough, 2017). Copy rights are reserved ELSEVIER B.V. 2017

Formation damage caused by injected water in Wolfcamp.

Water injection can cause problems if prior injection tests were not done properly. According to Zhong and Leung, fracturing fluids could cause water blockage. This water blockage will reduce gas relative permeability. This will affect gas production negatively, especially if near-well fractures are disconnected (Zhong & Leung, 2019). Similarly, Barati et al. stated in their study that as the formation get more saturated with water, gas relative permeability will be reduced and mechanical damage will occur. This could mean that fracture fluids may have been leaked off. As a result, capillary pressure will increase (Barati, et al., 2009).

Another problem that could arise from water injected and could harm Wolfcamp formation is phase trapping. Phase trapping is when oil is trapped in a porous media while drilling or completion is in progress. Reduction in effective permeability will be resulted from such a problem (Bennion, Thomas, Schulmeister, & Romanova, 2006).

Clay swelling is another issue to be aware of when injecting water. Because if low salinity water contacted the formation clay, the clay will flocculate or swell. The migration of these flocculated clay particle is the main cause of sensitive clay related formation damage (Donham, 1991).

Methodology

Decline curve analysis

Production data for 24 wells located in the Permian basin in Texas were extracted from University Land web page (University Lands, 2019). The data included month by month production of oil in barrels and gas in Mscf. After exporting the data, and using each well's API, injected water and proppant data were extracted from the Fracfocus data base (Fracfocus.org, 2011). Each well had a separate Microsoft Excel file with oil and gas production data included along with injected water and type of proppants as well.

Each excel file was uploaded on IHS Harmony and using segments, decline curve analysis (Arps method) (IHS decline plus, 2019) was conducted (Figure 6).

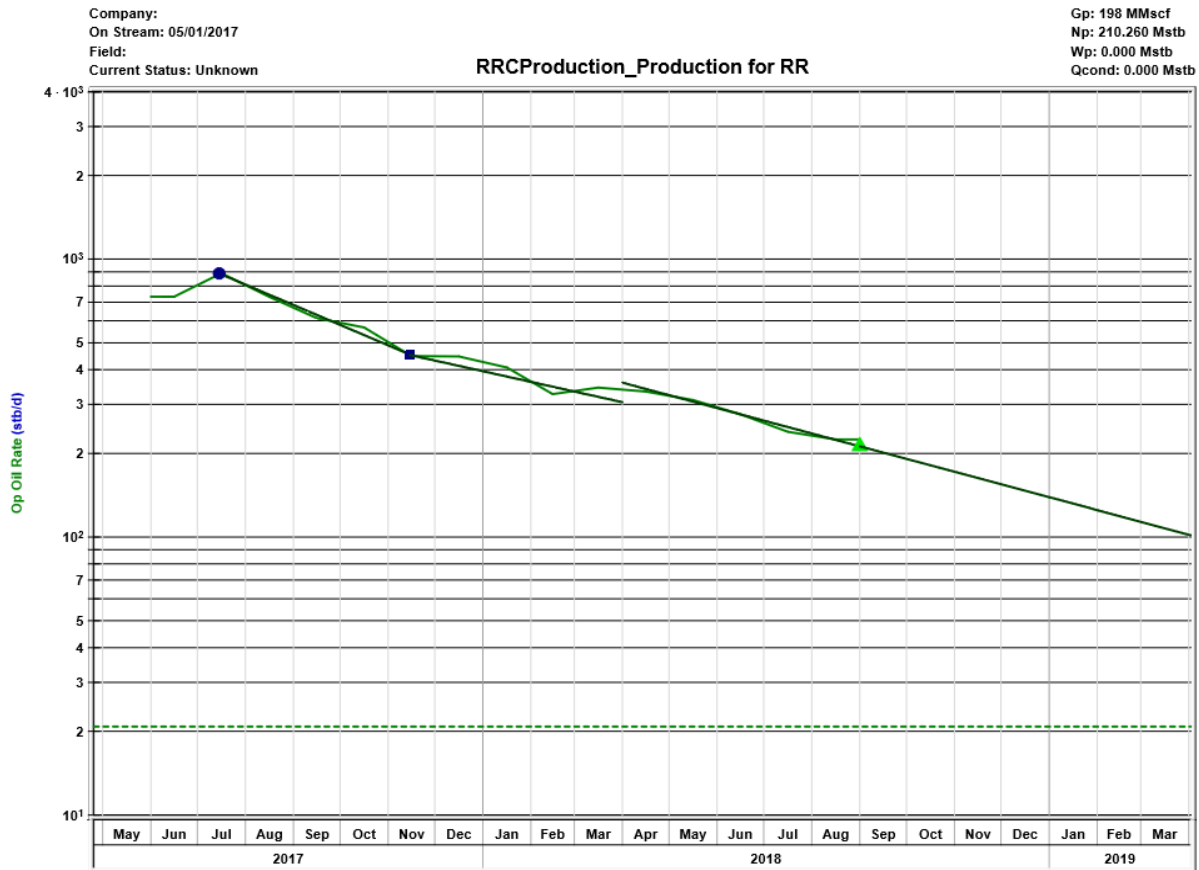


Figure 7 IHS Harmony, production data matching for well 23

What we get from Decline curve analysis after plotting production data vs time is a forecast of future production. Not only that, but also, we get estimated oil recovery of one or multiple wells as well as other information like water and oil volume. There are different methods used to analyze unconventional oil and gas production data (Clarkson C. R., 2013):

- Straight-line analysis method
- Type curve methods
- Analytical and numerical simulation

- Empirical method
- Hybrid method

Within the empirical method there are different models. Arps model is the most commonly used model for forecasting well performance. His model includes three methods (Arps, 1945):

1. Exponential decline
2. Hyperbolic decline
3. Harmonic model

All of the three models are solution of a differential equation (Barati & Aghababa, 2016):

Equation 1

$$D = \frac{\frac{dq}{dt}}{q} = -dq^b$$

Letter	What does it stand for
b	Nominal exponential decline rate
q	Production rate at time t

Exponential decline

b = 0	Decline exponent
Rate-time relationship: Equation 2 $q_t = q_i e^{-dt}$	where q_t is production rate at time t, and q_i is initial production
Cumulative-rate relationship: Equation 3 $Q_t = \frac{(q_i - q)}{d_i}$	where Q_t is cumulative production, and d_i is nominal decline rate

Hyperbolic decline

Hyperbolic decline is valid when b-value is between 0 and 1.

The decline/ rate-time relationship equation	Equation 4 $q_t = q_i(1 + bdt)^{-\frac{1}{b}}$
Cumulative-rate relationship	Equation 5 $Q_t = \frac{q_i^b}{d_i(1-b)}(q_i^{1-b} - q^{1-b})$
d_i relationship	Equation 6 $d_i = \left(\left(\frac{q_i}{q}\right)^b - 1\right) \div bt$

Harmonic decline

Harmonic decline is valid when b-value is = 1.

The decline equation	Equation 7 $q = \frac{q_i}{(1 + bt)}$
Cumulative-rate relationship	Equation 8 $Q_t = \frac{q_i}{d_i} \ln \frac{q_i}{q}$

d_i relationship	Equation 9 $d_i = \frac{\left(\frac{q_i}{q}\right) - 1}{t}$
--------------------	--

Doung Method

When it comes to tight or shale gas wells, Arps's rate-time model usually gives a highly optimistic EUR results. Doung presented a rate-decline analysis method that is applicable for reserves with dominant fracture flow and negligible matrix contribution. The rate vs time equation is presented as the following (Barati & Aghababa, 2016):

Equation 10

$$q = q_1 t^{-n}$$

Or can be presented as follows:

Equation 11

$$q = q_1 * t^{-m} e^{\frac{\alpha}{1-m}(t^{1-m}-1)} + q_{\infty}$$

Cumulative production equation	Equation 12 $Q_t = \left(\frac{q_1}{a}\right) * e^{\frac{\alpha}{1-m}(t^{1-m}-1)} + q_{\infty} t$
Ratio	Equation 13 $\frac{q}{Q_t} = a t^{-m}$

Segment analysis technique:

Conventional and unconventional resources have different behavior when it comes to decline curve analysis. Unconventional shale resources are known with their low permeability; therefore,

advanced drilling and completion techniques are needed. Production profile is the main thing to look for in evaluating the resource. Arps and Doung methods are used in unconventional resources. In unconventional shale resources, usually the decline exponent in Arps's model is greater than 1 (Barati & Aghababa, 2016).

Depend on how smooth the curve is, each well had different number of segments to ensure accuracy in the analysis. Most wells had 3 segments, some though needed 5. After analyzing the data, 4 coefficients were extracted from Harmony into excel again. These 4 coefficients are Q_i , D_i , t , and b . Q_i represents the cumulative production at the start of the forecast. D_i is the effective secant decline rate at the start of the forecast. B is the decline exponent and t is the duration of the forecast. Each segment had a separate Arps parameter. Therefore, a graph was made on excel for each segment that included all the 24 wells injected water volume vs each of the 4 coefficients. A total of 20 graphs were made for the 5 segments. The same was done for the proppant for each segment vs each of the 4 coefficients.

A forecast of oil and gas production was made for each well. Forecasting production in harmony is based on history matching where production data of the previous years are matched using segments and the forecast data are obtained using Arps equation with parameters that were estimated by the segments matching.

CMG model

Reservoir properties and PVT data

Table 1 PVT data

Fracture width	0.001ft
Fracture permeability	10md
Half-length	100ft

Number of layers above perforation	3
Number of layers below perforation	3
Grid cell width	2ft
Grid thickness	20ft
Matrix porosity	0.06
Fracture Porosity	0.001
Matrix permeability in I and J direction	0.005md
Fracture permeability	Between 0.1 up to 100md
Water saturation	0.4 for all models and between 0.45 to 0.55 for representative models
Pressure	5,000 psi
Reservoir temperature	110 F
Oil density	50.863 lb/ft ³
Gas gravity	0.7
Viscosity	0.8cp
Compressibility	3.17118e-6 1/psi
Reference pressure for formation volume factor	14.696
Formation volume factor	1.00805

SCAL

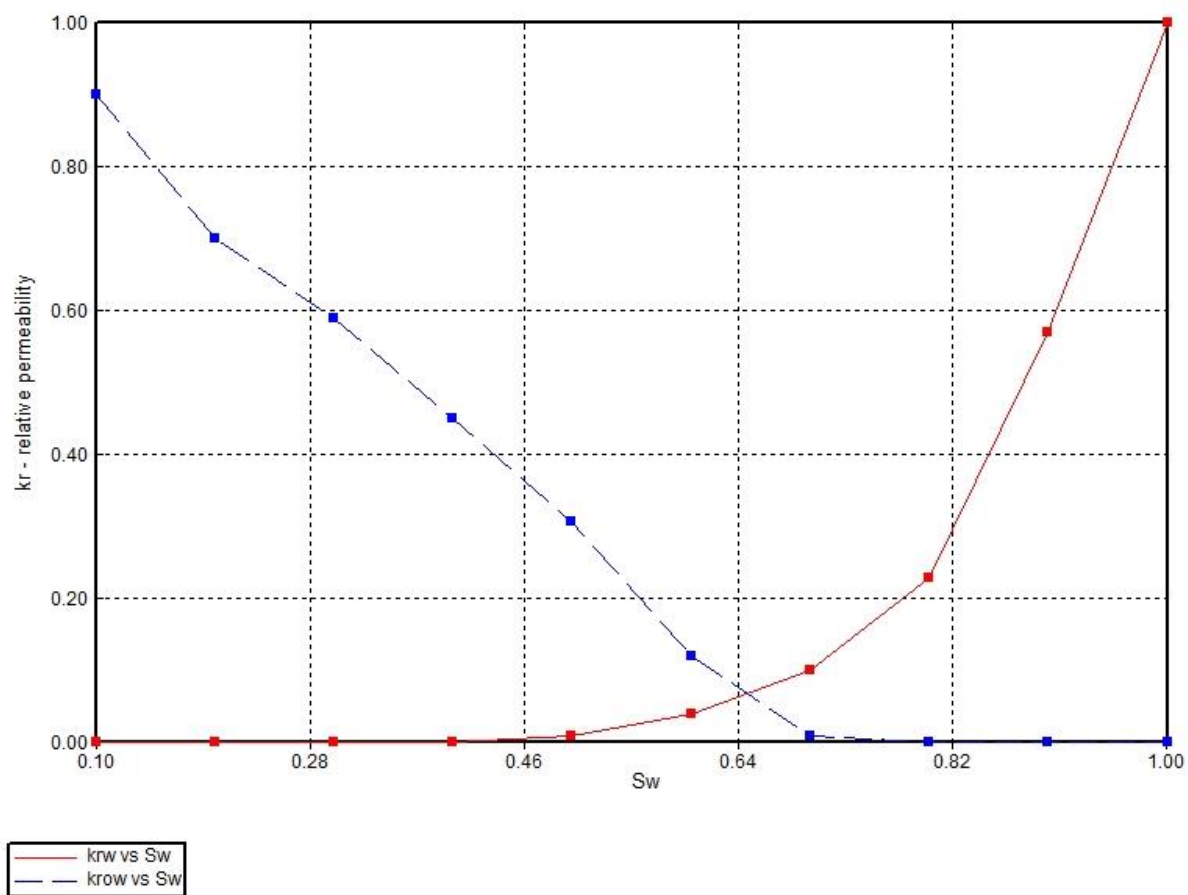


Figure 8 Oil-water relative permeability curve

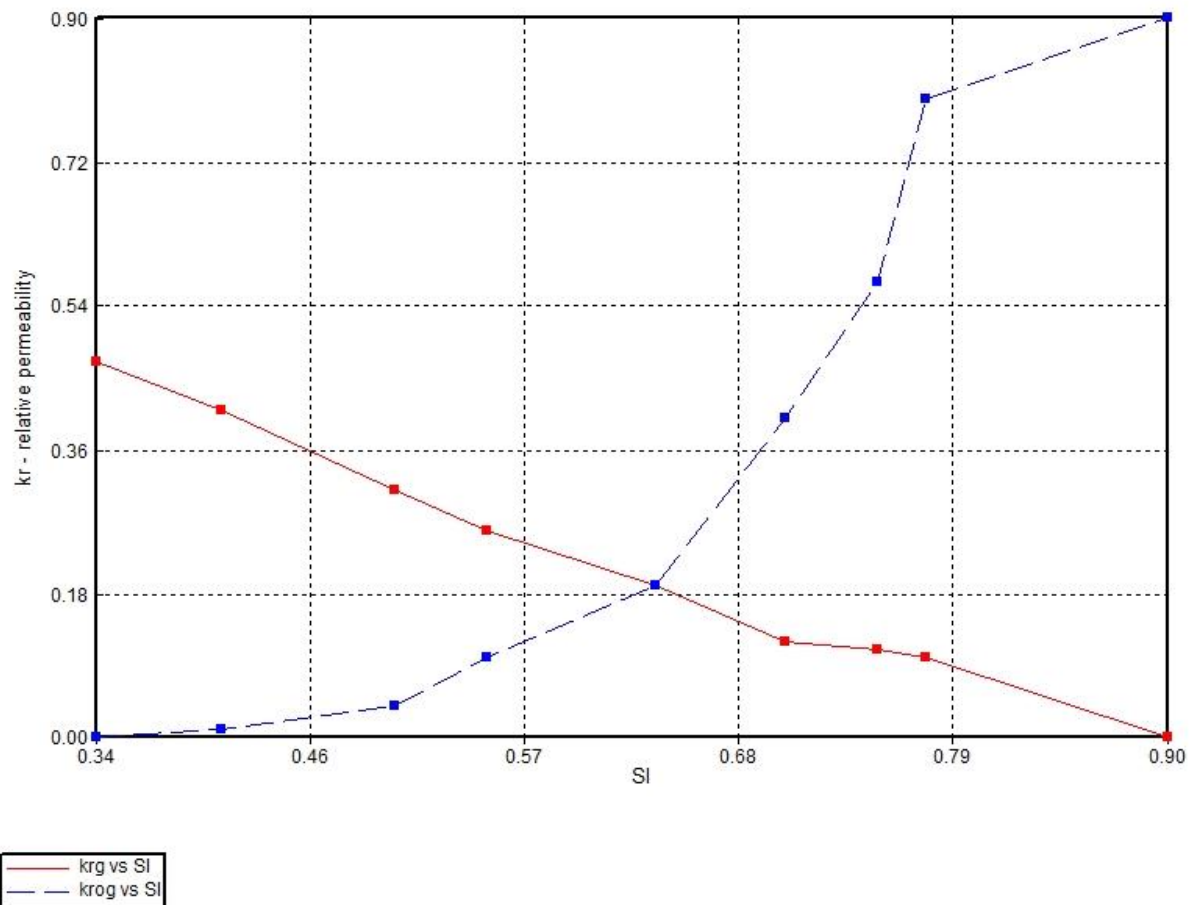


Figure 9 gas-oil relative permeability vs liquid saturation curve

Figure 7 is a representation for oil-water relative permeability curve where the water relative permeability vs water saturation is shown where K_{rw} is the water relative permeability and K_{row} is oil relative permeability. Figure 8 is gas-oil relative permeability curve.

Both relative permeability graphs was extracted from previous studies and papers published by (Ojha, et al., 2018).

Table 2

Porosity	6%	(Gupta, Rai, Sondergeld, & Devegowda, Rock Typing In Wolfcamp Formation, 2017)
Depth of formation	Between 7,750 and 8,000 ft	(Gupta, Rai, Sondergeld, & Devegowda, Rock Typing In Wolfcamp Formation, 2017)
Pressure	6,000	(Ojha, et al., 2018)
Initial water saturation	0.4	(Forrest, Zhu, Xiong, & Pradhan, 2018)
Relative permeability curve		(Ojha, et al., 2018)

Permeability effect

At the beginning 3 main models were made in CMG Builder. Builder is an application in CMG where reservoir models are created in CMG. The three models had the exact same properties and the only difference was the fracture half-length. The first model had a fracture half-length of 100ft. The second and third model had fracture half-length equal to 200ft and 350ft, respectively. Each of the three models were duplicated 4 times where permeability was the only thing changed. The models started with fracture permeability equal to 0.1md and elevating until it reached 100md where each model had 10x the permeability of the previous one. The process was repeated for each model with different fracture half-length. For example, the first four models had $X_f = 100\text{ft}$ and $k = 0.1, 1, 10, \text{ and } 100\text{md}$.

Table 3 Models' fracture half-length and permeability

Model number	Permeability
Model 1 ($X_f = 100\text{ft}$)	0.1md
Model 2 ($X_f = 100\text{ft}$)	1md
Model 3 ($X_f = 100\text{ft}$)	10md
Model 4 ($X_f = 100\text{ft}$)	100md
Model 5 ($X_f = 200\text{ft}$)	0.1md
Model 6 ($X_f = 200\text{ft}$)	1md
Model 7 ($X_f = 200\text{ft}$)	10md
Model 8 ($X_f = 200\text{ft}$)	100md
Model 9 ($X_f = 350\text{ft}$)	0.1md
Model 10 ($X_f = 350\text{ft}$)	1md
Model 11 ($X_f = 350\text{ft}$)	10md
Model 12 ($X_f = 350\text{ft}$)	100md

Water saturation effect

After seeing the effect of permeability on oil and gas production, we wanted to test the effect of water saturation. As the fracture half-length of a well increases it allows more water to be injected and will increase the amount of water in place near fracture zone which will make the formation more saturated with water. Therefore, each model had different water saturation depending on its fracture half-length. We have selected 3 representative models and changed a few of other parameters except the fracture half-length. The first model had S_w equal to 45%.

This model had the lowest permeability among the 3 models with a fracture permeability equal to 5md. Its X_f is still 100ft.

The second model with the 200ft fracture half-length had a permeability of 10md. This model's water saturation was 50%. The last model where fracture half-length was 350ft had a permeability of 20md. This model was given the highest as well as the highest water saturation with $S_w = 55\%$

Table 4 Models properties

Model number	Permeability	Water saturation
Model 1	5md	45%
Model 2	10md	50%
Model 3	20md	55%

Optimum fracture half-length

After seeing the results for the three models we wanted to be precise more. So a new model was created that had $X_f = 250$ ft, $k = 10$, and water saturation of 51.5%. The goal for creating this model is to see the peak for oil and gas production by changing fracture half-length and water saturation.

Capillary pressure effect

In this set of models, we copied the work that was done in the previous set and modified one thing. Capillary pressure was added to the 3 models. All models had the exact same trend of capillary pressure and it varied between 0 to 100 psi on 10 steps shown in table 1.

Table 5 Water saturation vs Capillary pressure

Sw	Pc, Psi
0.5	100
0.6	75
0.7	35
0.8	18
0.9	5
1	0

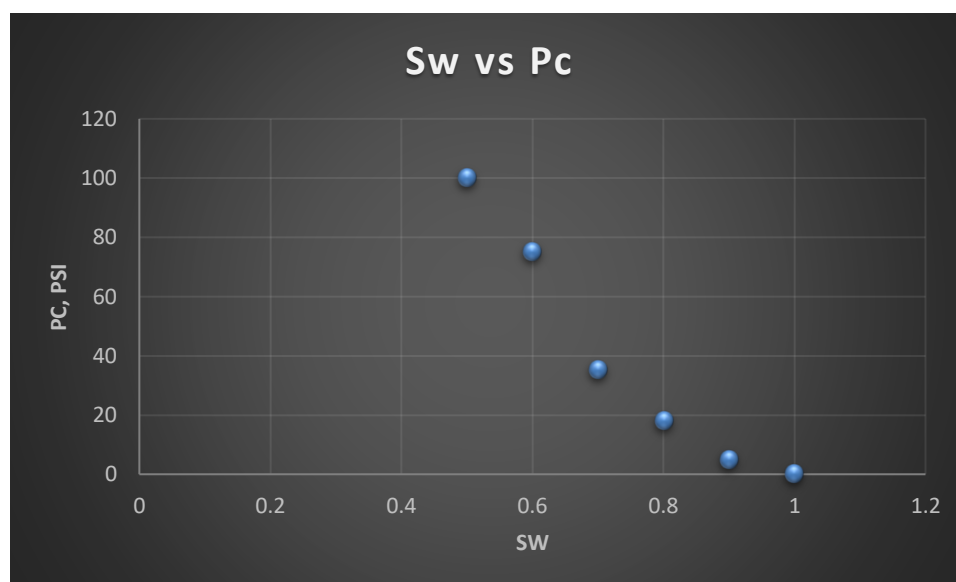


Figure 10 Water saturation vs Capillary pressure

Economic Analysis

A full economic analysis was made for the three representative models. The production data that we got from CMG was exported to Microsoft Excel. A month by month cumulative production data was available for oil, gas, and water. Produced water was assumed to be 60% of the injected water and that's how we got the injected water volume. This volume was multiplied by \$0.35 to estimate the cost of buying fresh water. According to Scanlon the cost of one barrel of fresh or

brackish water is \$0.35 and the cost to dispose this water is between \$0.5 without transporting it up to \$2 with transportation for one barrel (Scanlon, Reedy, Male, & Walsh, 2017). The chosen price for water disposal was \$1.5 including transportation. This number was multiplied by the amount of produced water and that will be water disposal cost. Water buying and disposing price were added toward the expenses in the budget sheet. The same article assumes that the cost for drilling and completion for a well in the Permian Basin is ranged between \$6.6MM to \$7.8MM. QEP Resources estimate oil lift price in the Permian basin to be between \$0.5 to \$1.00/bbl so we chose the value in between \$0.75/bbl. All expenses were added up for each case and recorded. We assumed then the oil price to be \$50/bbl and we multiplied this number with the monthly production. The same was done for gas with a price of \$3.00/MSCF. Each month's revenue (for oil + gas) was subtracted from the expenses to notice when will the company breakeven and starts making profit. The equations for this analysis are demonstrated below:

$$\text{Injected water volume} = \frac{\text{Produced water volume}}{0.6}$$

$$\text{Injected water cost} = \text{Injected water volume} \times \$0.35$$

$$\text{Water disposal price} = \text{Produced water volume} \times \$1.5$$

$$\text{Oil lift cost} = \text{Cumulative oil production} \times \$0.75$$

All expenses were added along with drilling a well cost which was \$7.8MM

$$\text{Oil revenue} = \text{Cumulative oil production} \times \$50$$

$$\text{Gas revenue} = \text{Cumulative gas production} \times \$3.00$$

Internal rate of return or IRR was calculated as well to see which project breaks even faster. The IRR is basically a way to measure profitability of prospect investment. To calculate IRR, multiple steps should be followed. The present value should be calculated first. The equation used to calculate the present value (PV) is calculated as follows:

$$PV = Future\ Value \times \left[\frac{1}{(1 + i)^n} \right]$$

where,

i = interest rate

n = number of periods

The interest rate was 15% and the number of period was 0 for the beginning where all expenses were paid, 1 after the first 12 months, 2 after the next 12 months, and 3 for the last 12 months. After calculating the present value, net present value (NPV) was calculated. NPV is the summation of the PV of the profitable years minus the expenses, which basically means in our case, the profits made in the 3 years minus the expenses paid at the beginning and during the time of the project. Internal rate of return was calculated in Microsoft Excel. Excel has a function that will calculate IRR and basically the equation for IRR is setting the NPV equals to the value of zero.

Due to lack of demand nowadays for natural gas in the Permian basin, companies are losing money by producing gas and not selling it. This process cost money and companies are required by law to dispose the natural gas if it was not sold. So, another scenario was created where instead of getting revenues from gas, gas production is considered as an additional cost to the expenses. Assuming that disposing this gas cost \$0.5 another scenario was created that affected the net cash flow and IRR and will be demonstrated further in the result.

Results and discussion

DCA – Decline curve analysis

Starting with the decline curve analysis and based on the production data we had from University Lands website (University Lands, 2019) the trend shows an increase in oil and gas production as more and more water was injected. The well with the lowest injected water had the lowest Q_i and the well with the highest injected water had the highest Q_i as shown in figures 10 through 13 and figures 44 through 59. To test if this is always the case, few models were made using CMG applications that will stimulate the well.

Since some wells had low quality data, some segments in few wells were not very accurate, therefore it might have affected the Q_i for that specific segment. Others were more than 90% accurate. Figures 10 through 13 will show the graph for the first segment injected water volume versus each of the 4 coefficients in Arps equation. In the first segment for example, Q_i is increasing as more water is injected. Figures 44 through 59 will show the graphs for other segments

First segment graphs

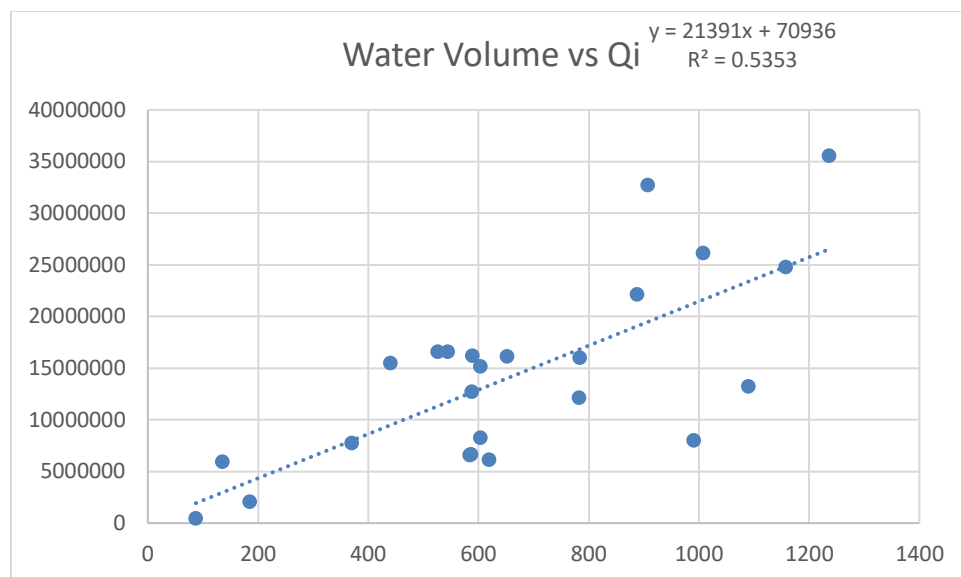


Figure 11 Injected water volume in Gal vs Qi

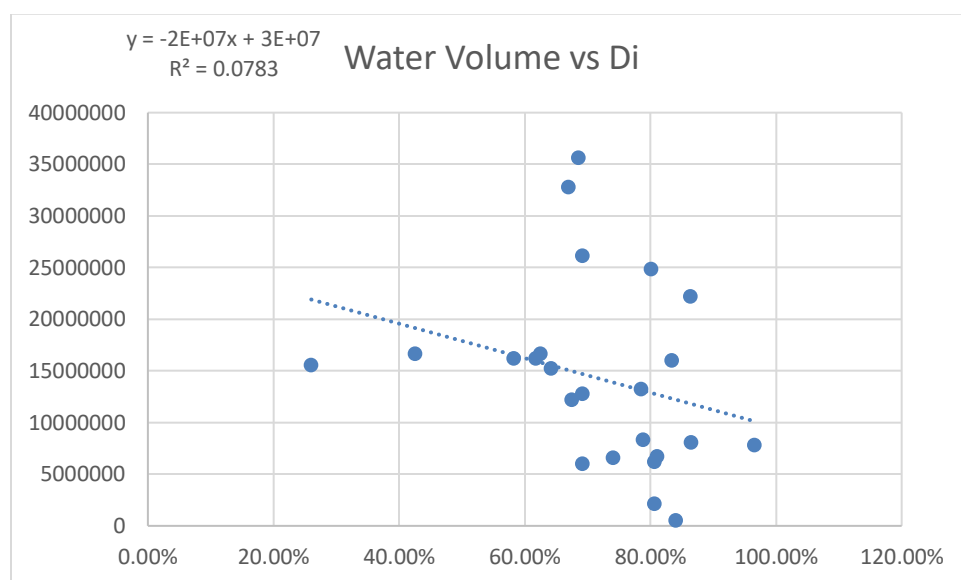


Figure 12 Injected water volume in Gal vs Di

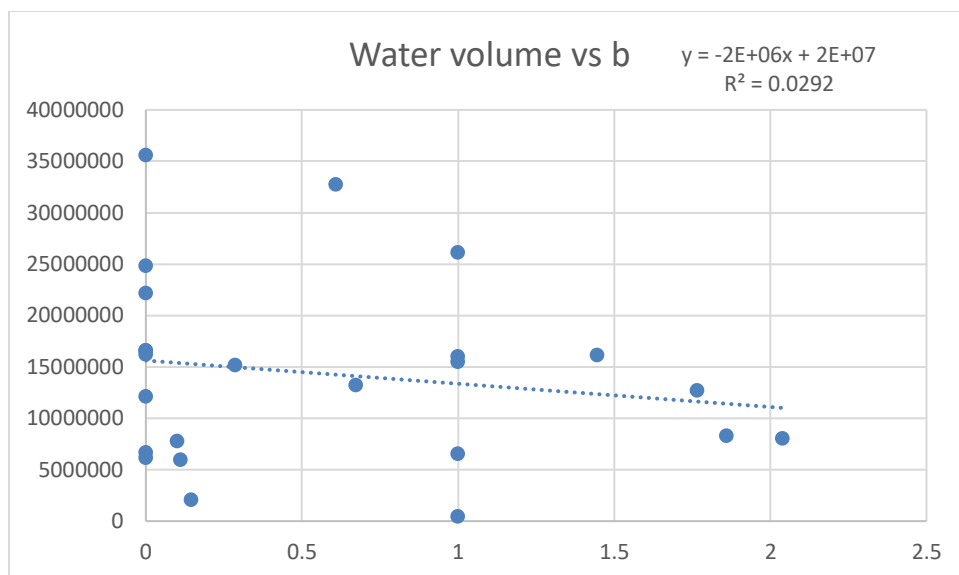


Figure 13 Injected water volume in Gal vs b

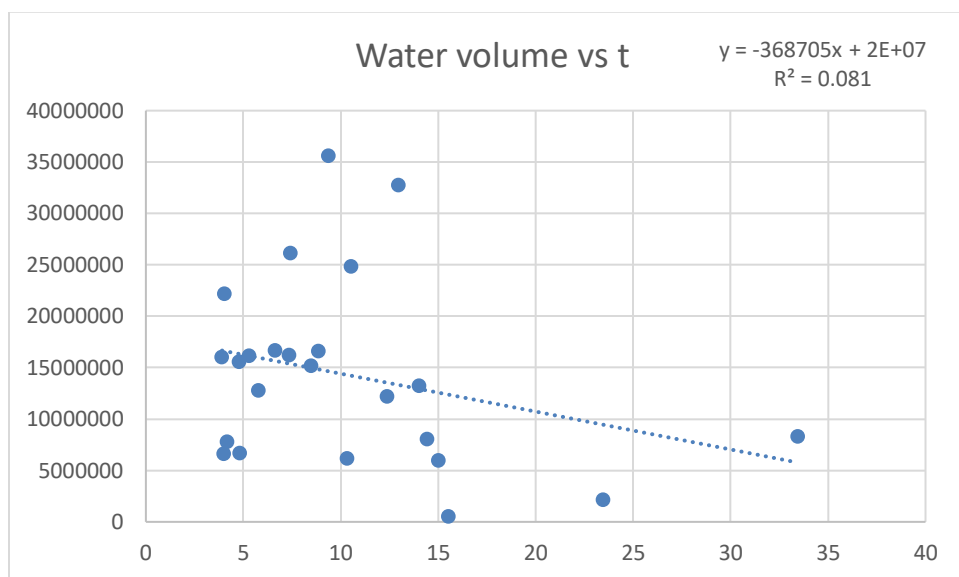


Figure 14 Injected water volume in Gal vs time in months

CMG models

The purpose for CMG modeling is to stimulate reservoirs and test before applying our simulation in real wells. For example, instead of drilling three wells in one formation with different fracture half-length, to see which well will be the most productive, we could test that in three CMG models. All the data used in these models are real data based on previous drilled wells in the same formation.

Effect of fracture permeability

CMG models were created to conduct sensitivity analysis and investigate the effect of injected water as well as fracture length on the production of wells. The first model fracture half-length was 100ft. Fracture permeability was 0.1, 1, 10, or 100md. Production graph was captured and is displayed below in Figure 9

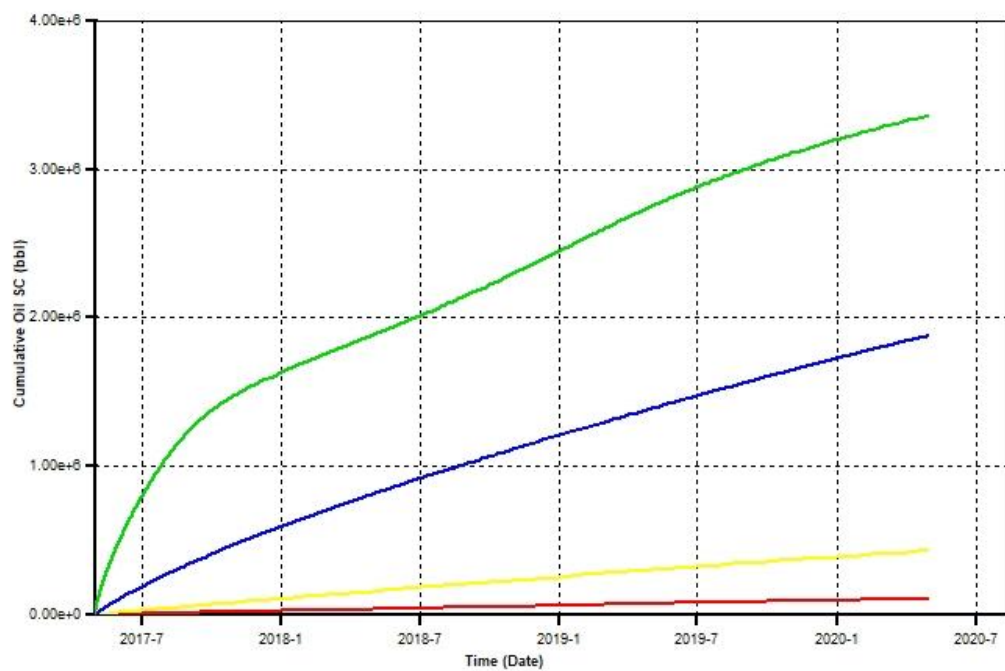


Figure 15 Cumulative oil production for the first model, comparing different fracture permeability.

$k = 0.1\text{md}$

$k = 1\text{md}$

$k = 10\text{md}$

$k = 100\text{md}$

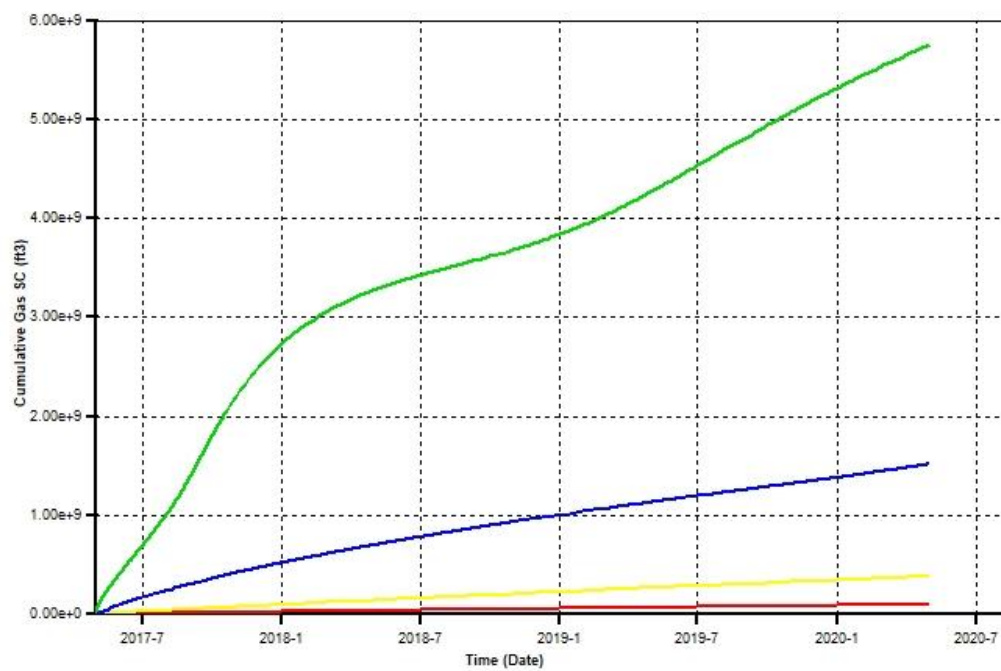


Figure 16 Cumulative gas production for the first model comparing different fracture permeability

$k = 0.1\text{md}$

$k = 1\text{md}$

$k = 10\text{md}$

$k = 100\text{md}$

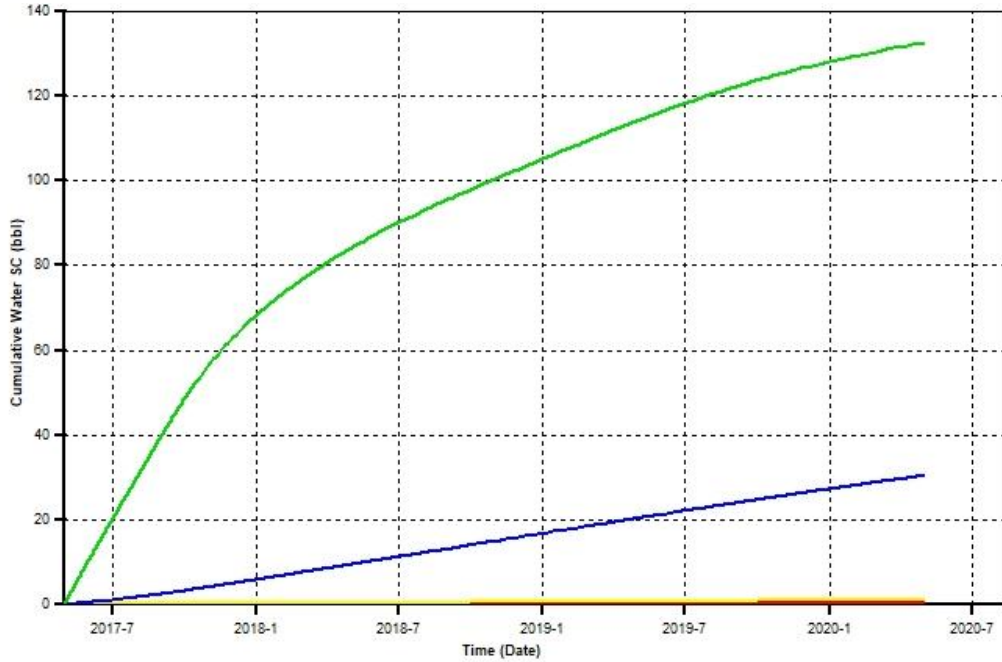


Figure 17 Cumulative water production for the first model comparing different fracture permeability

$k = 0.1\text{md}$

$k = 1\text{md}$

$k = 10\text{md}$

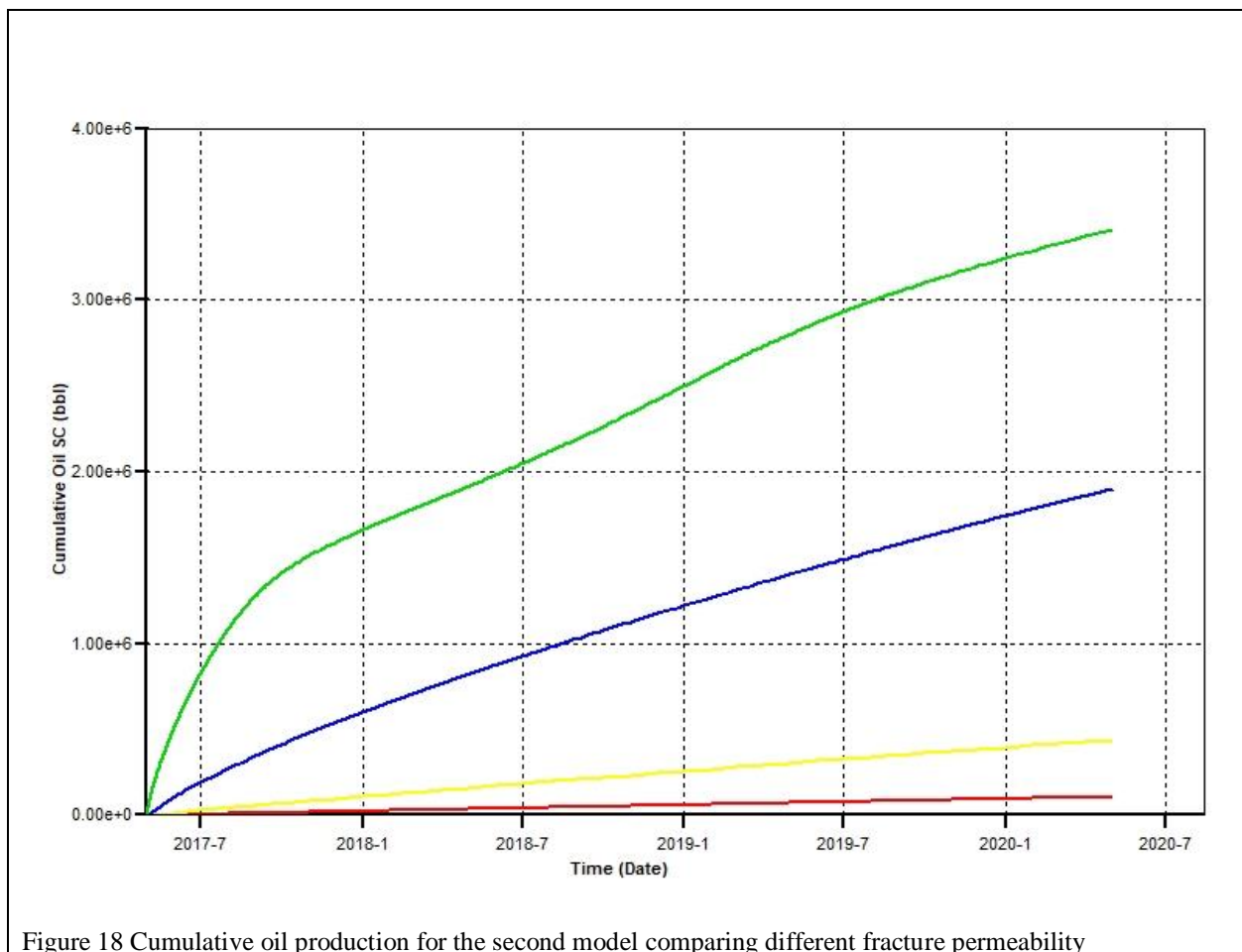
$k = 100\text{md}$

Table 6 oil, gas, and water production for the first model

Permeability	Oil production, res bbl	Gas production, MSCF	Water production, res bbl
K = 0.1md	$1.1e^5$	$9.8e^4$	6
K = 1md	$4.4e^5$	$3.85e^5$	8
K = 10md	$1.85e^6$	$1.5e^6$	36
K = 100md	$3.3e^6$	$5.8e^6$	134

The highest oil and gas production was for the well with the highest fracture permeability. The reason is because permeability reflects the ability of movement of oil, gas, or water through a formation (AAPG wiki, 2016), Therefore, higher fracture permeability means an easier flow for oil and gas through the fracture towards production zone which means more production. As permeability decreases oil and gas production significantly decreased as shown in the figures 9 and 10.

In the second model, X_f was 200ft. k was the same as the previous model. Results of this model were the most optimistic. Figure 12 through 14 will demonstrate more:



$k = 0.1\text{md}$

$k = 1\text{md}$

$k = 10\text{md}$

$k = 100\text{md}$

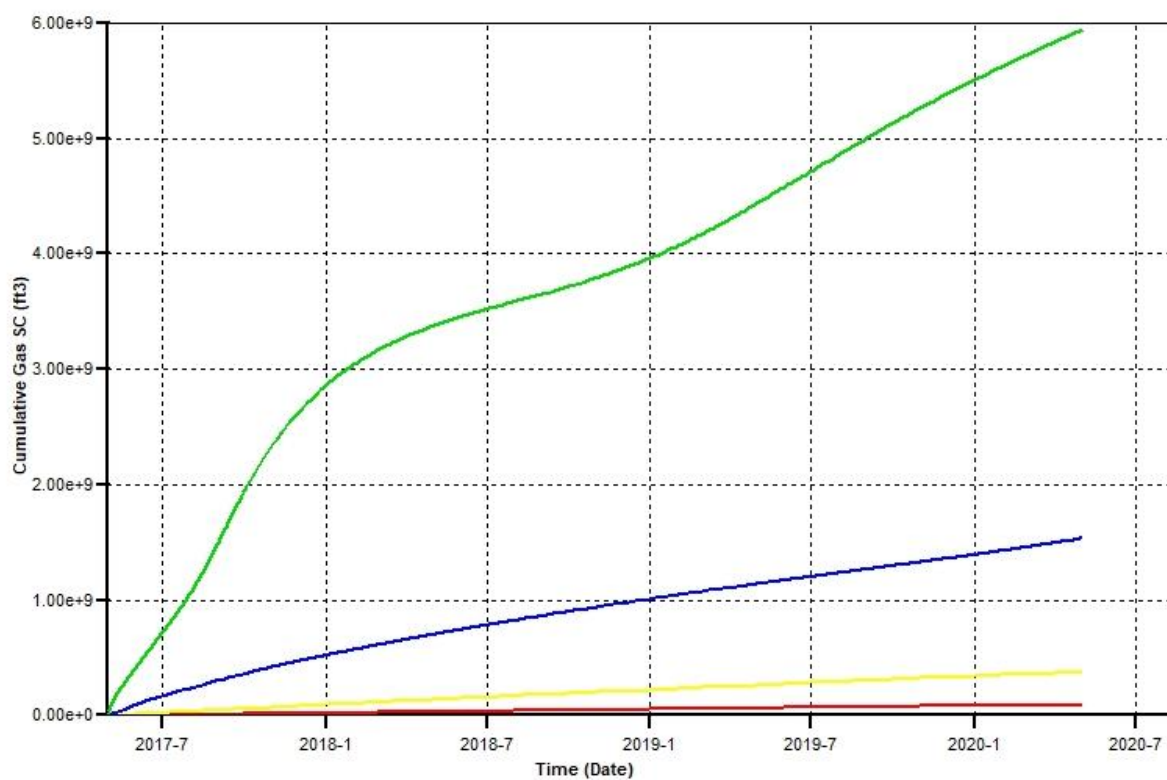


Figure 19 Cumulative gas production for the second model comparing different fracture permeability

$k = 0.1\text{md}$

$k = 1\text{md}$

$k = 10\text{md}$

$k = 100\text{md}$

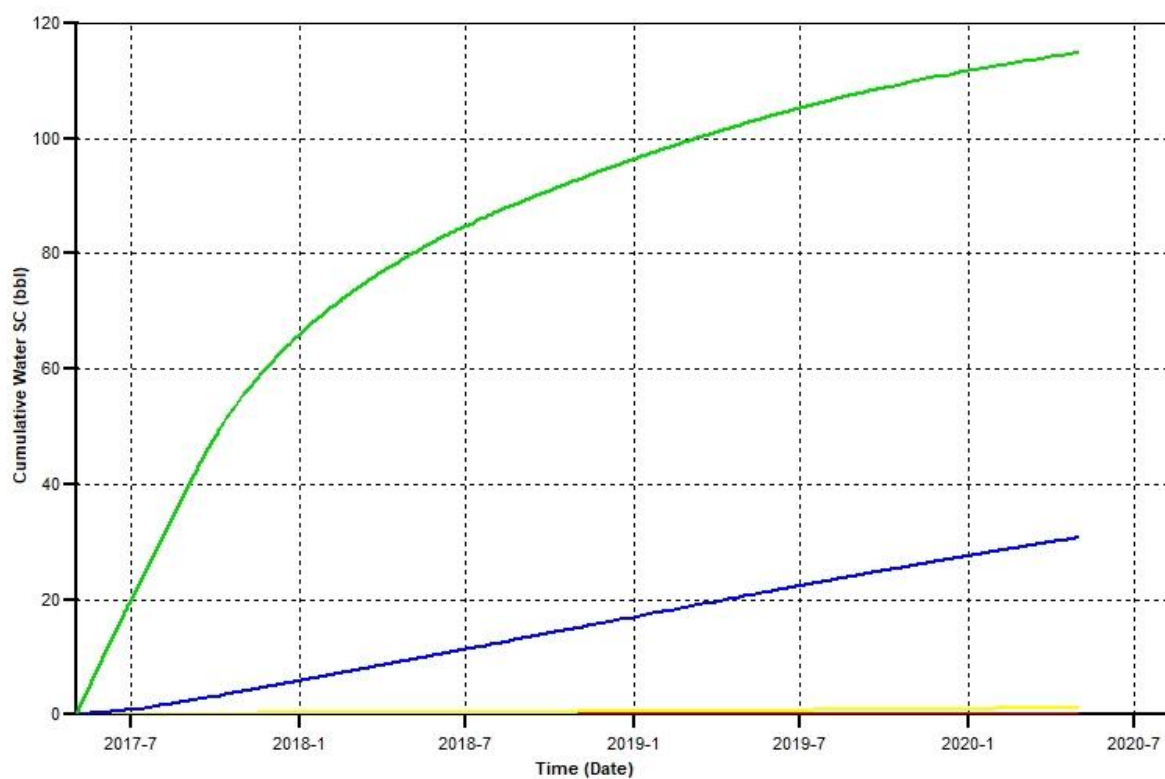


Figure 20 Cumulative water production for the second model comparing different fracture permeability

$k = 0.1\text{md}$

$k = 1\text{md}$

$k = 10\text{md}$

$k = 100\text{md}$

Table 7 Oil, gas, and water production for the second model

Permeability	Oil production, Res bbl	Gas production, MSCF	Water production Res bbl
K = 0.1md	$1.1e^5$	$1e^5$	6
K = 1md	$4.4e^5$	$3.5e^5$	8
K = 10md	$1.9e^6$	$1.6e^6$	32
K = 100md	$3.4e^6$	$6e^6$	118

Since the only difference between this model and the other models is the fracture half-length, it is assumed that 200ft is the best option between 100ft and 350ft for fracture half-length in the Wolfcamp formation. Further test will be done.

The last set of models were interesting. With fracture half-length equal to 350ft and the same permeability as the previous model, oil and gas production were almost the same with the previous models. Assuming that water saturation was the same, and no formation damage occurred. The following graph will demonstrate further:

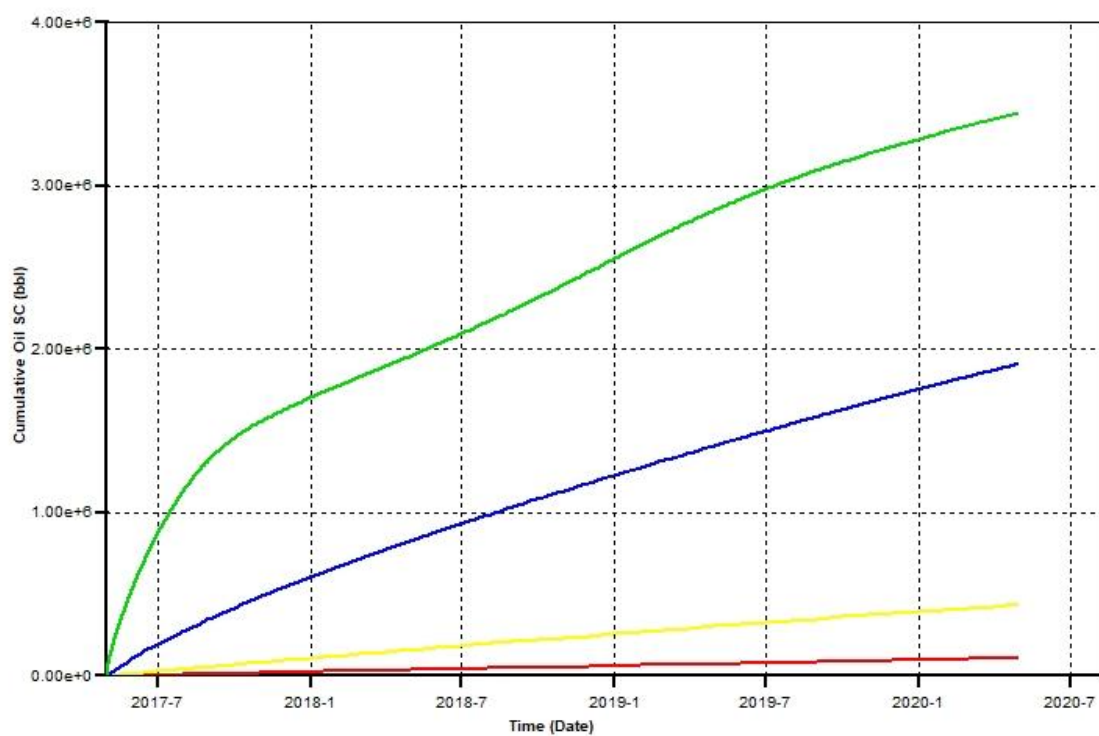


Figure 21 Cumulative oil production for the third model comparing different fracture permeability

$k = 0.1\text{md}$

$k = 1\text{md}$

$k = 10\text{md}$

$k = 100\text{md}$

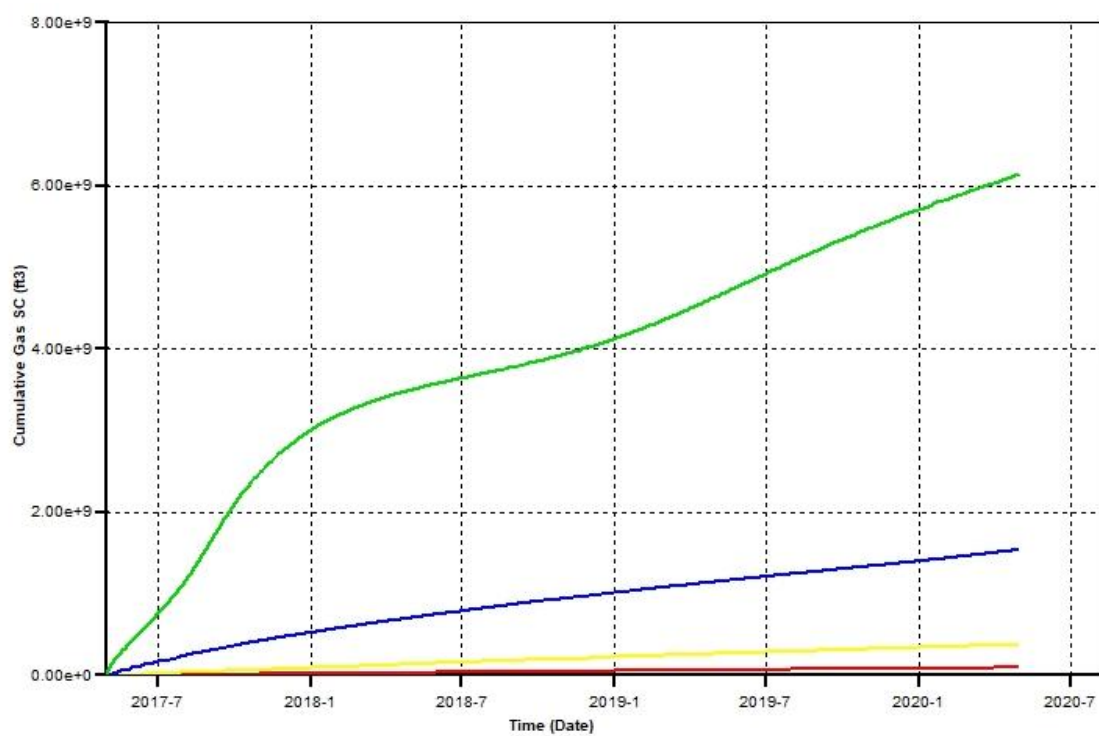


Figure 22 Cumulative gas production for the third model comparing different fracture permeability

$k = 0.1\text{md}$

$k = 1\text{md}$

$k = 10\text{md}$

$k = 100\text{md}$

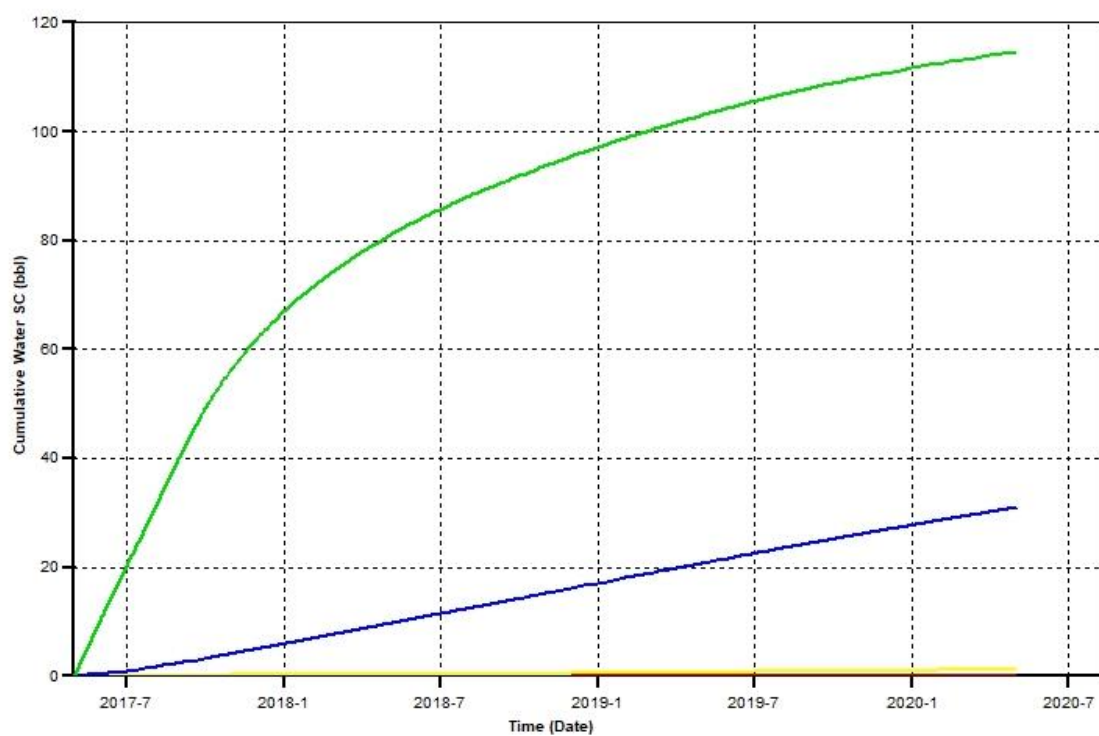


Figure 23 Cumulative water production for the third model comparing different fracture permeability

$k = 0.1\text{md}$

$k = 1\text{md}$

$k = 10\text{md}$

$k = 100\text{md}$

Table 8 Oil, water and gas production table for the third model

Permeability	Oil production, res bbl	Gas production, MSCF	Water production, res bbl

K = 0.1md	$2e^5$	$2e^5$	6
K = 1md	$4.6e^5$	$4e^5$	8
K = 10md	$1.9e^6$	$1.7e^6$	34
K = 100md	$3.5e^6$	$6.2e^6$	137

Effect of water saturation

To test the effect of water saturation we created three models with the exact same properties and changed water saturation in each. The three models' fracture half-length was 200ft. fracture permeability for both models were 10md. Both models didn't have any capillary pressure added. Water saturation was 45% on the first one and 50% on the second one. The last model had water saturation of 55%. Oil and gas production graphs for each model are available in figure through

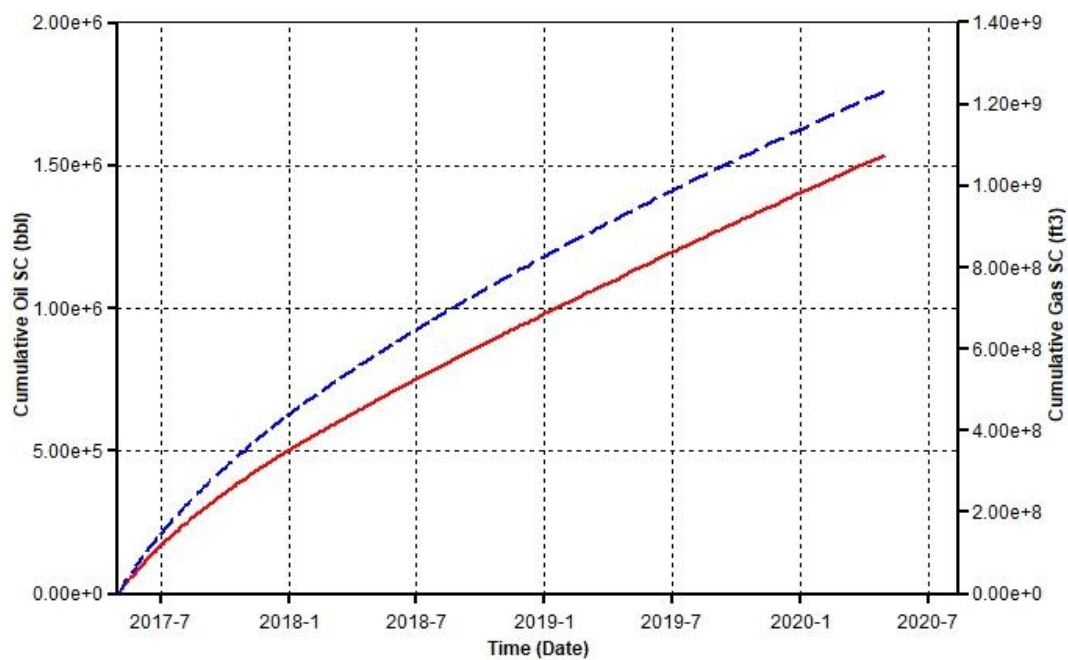
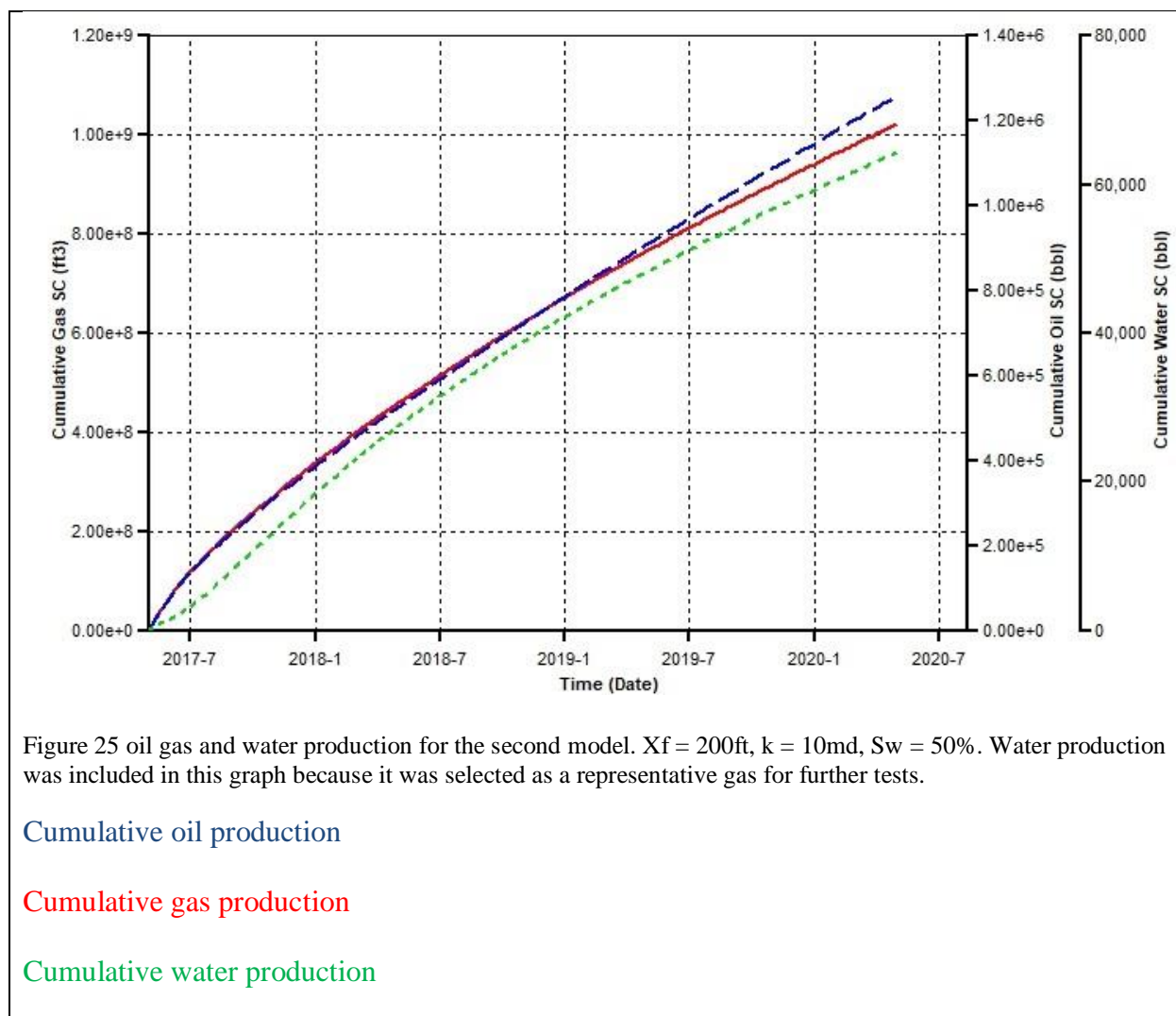


Figure 24 Oil and gas production for the first model. $X_f = 200\text{ft}$, $k = 10\text{md}$, $S_w = 45\%$

Oil curve

Gas Curve



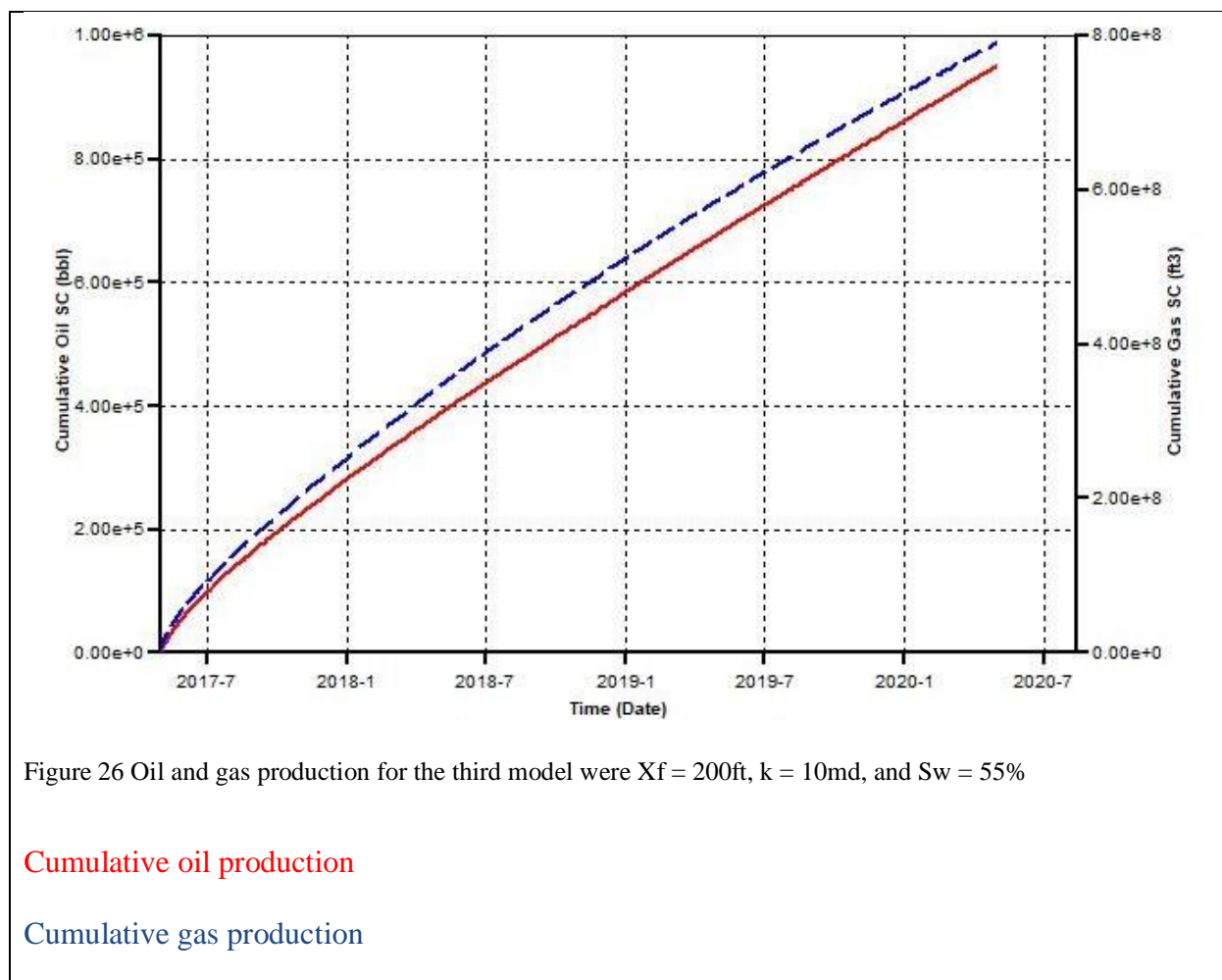


Table 9 Effect of water saturation

Model	Oil production in res bbl	Gas production in MSCF
$S_w = 45\%$	$1.51e^6$	$1.22e^6$
$S_w = 50\%$	$1.26e^+6$	$1.02e^6$
$S_w = 55\%$	$9.6e^5$	$8e^5$

Effect of Invaded water volume and Fracture Length on Production

Three models were selected from the previous step. Each of the three models had different fracture half-length and different fracture permeability simulating different volumes of water

injected and fractures propagated. Water saturation was added to these models to test the effect of injected water volume on oil and gas production. The first model which has X_f equal to 100ft and water saturation of 45%. The fracture permeability that was chosen for this model was 5md. The second model which has X_f equal to 200ft had water saturation of 50%. The permeability for this model was 10md. Finally, the third model had X_f equal to 350ft. Water saturation for this model was 55% and permeability was 20md. The graphs below show oil, gas, and water production, respectively, of the 3 representative models and the water saturation map will be attached in the figures section:

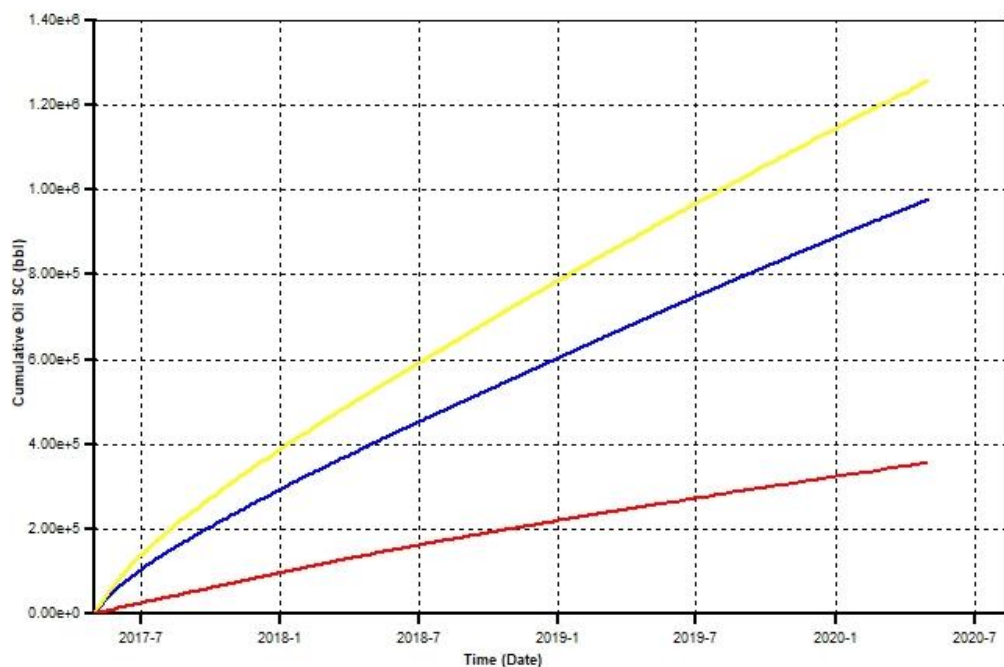


Figure 27 Cumulative oil production for the 3 representative models comparing different water saturation

$X_f = 100\text{ft}$, $k = 5\text{md}$, $S_w = 45\%$

$X_f = 200\text{ft}$, $k = 10\text{md}$, $S_w = 50\%$

$X_f = 350\text{ft}$, $k = 20\text{md}$, $S_w = 55\%$

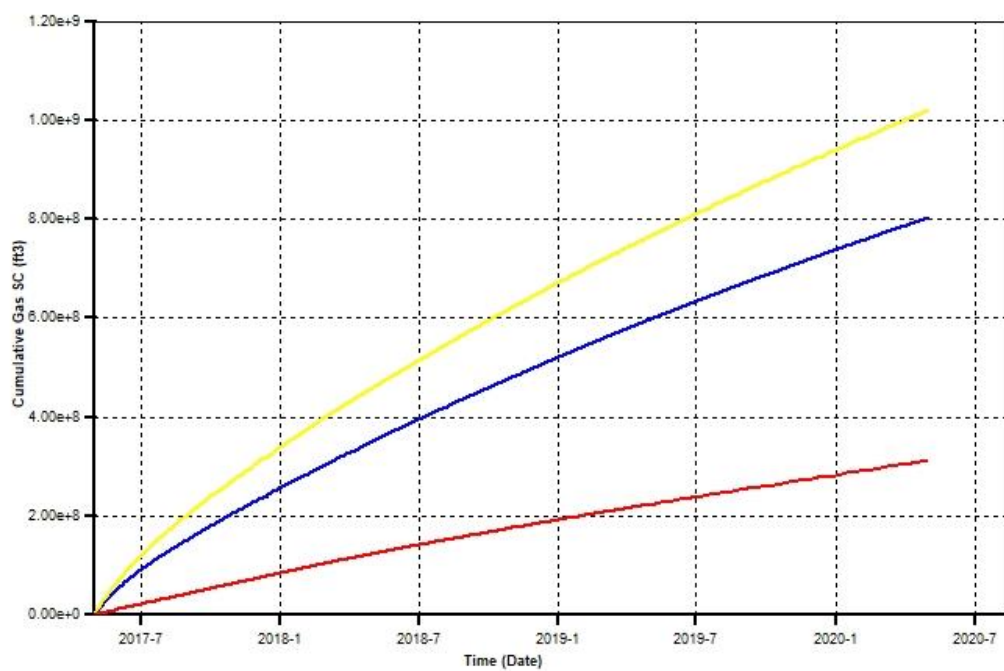
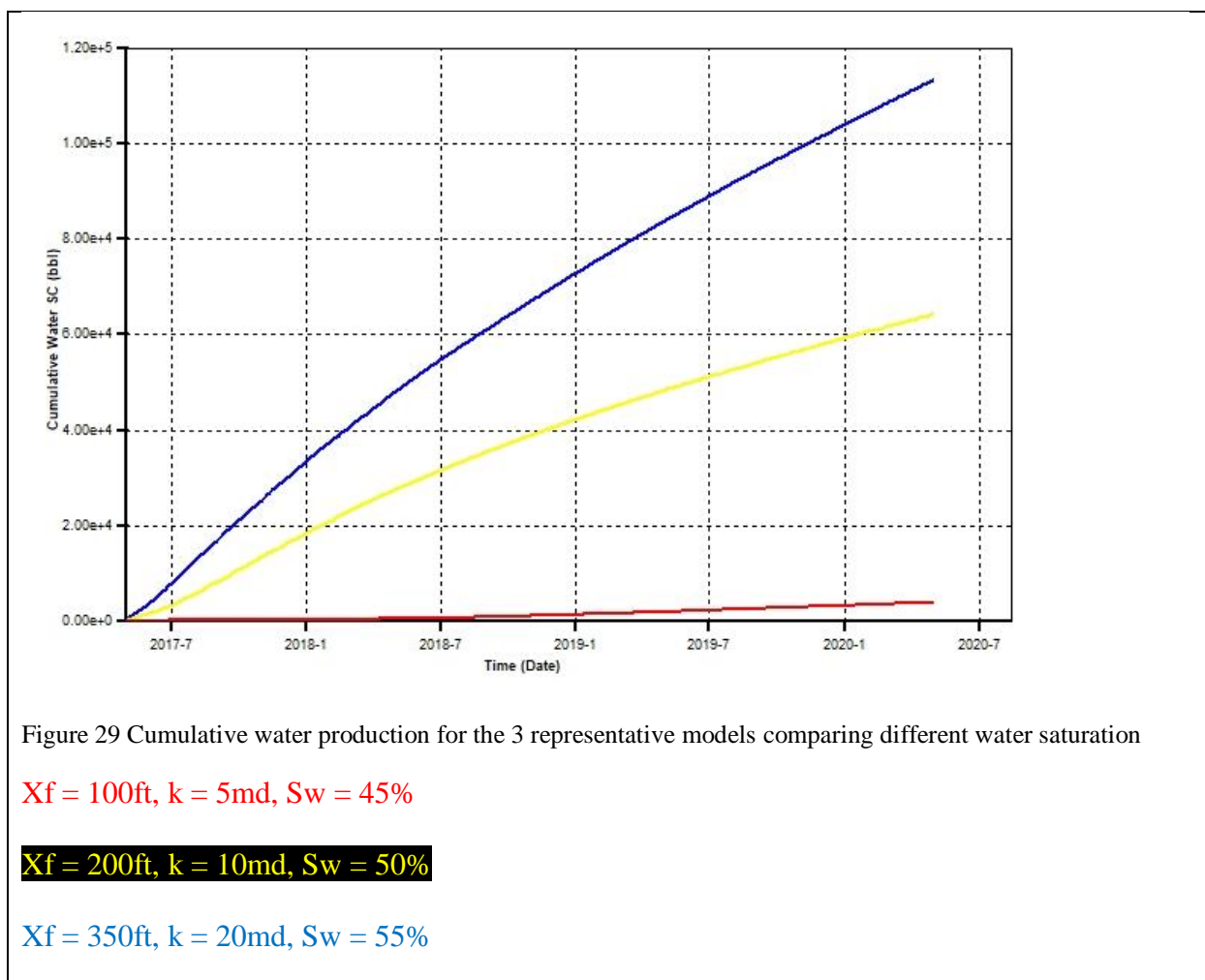


Figure 28 Cumulative gas production for the 3 representative models comparing different water saturation

$X_f = 100\text{ft}$, $k = 5\text{md}$, $S_w = 45\%$

$X_f = 200\text{ft}$, $k = 10\text{md}$, $S_w = 50\%$

$X_f = 350\text{ft}$, $k = 20\text{md}$, $S_w = 55\%$



Simulation results showed that the highest oil and gas recovery belonged to the second model with the 10 md permeability. What is surprising in the results is that the third model had twice as much of permeability and almost twice as much of fracture half-length. With an increase of 20% in oil and gas production the model with the lower permeability, fracture half-length, and water saturation dominates the model with the higher parameters. After some readings, Rail Road Commission of Texas states in their website that the optimum fracture half-length for Wolfcamp A & B (the two most productive formations) was ranged between 210-252ft (Railroad Commission of Texas, 2014). According to (Tayong A, Alhubail, Maulianda, & Barati, 2019) Increasing water saturation will result in hydraulic damage in pores around the fracture face.

This will reduce relative permeability of gas and could impede oil and gas flow during recovery.

It also could cause mechanical damage where production zones are damaged which will only help reducing hydrocarbon production (Barati, et al., 2009).

In regards with water production, even though the increase in water saturation is insignificant, we can see a dramatic increase in cumulative water production between the three models. When water saturation was 45%, cumulative water production didn't exceed 4,000 bbl. In the second model where water saturation is 50%, cumulative water production increased by more than 1500%. We can notice also a 188% increase of cumulative water production in the third model comparing to the second model. The table below will show in numbers a rough estimate for the cumulative oil, gas, and water production for all representative models.

	1 st model	2 nd model	3 rd model
Cumulative oil production in res bbl	$3.6e^{+5}$	$1.26e^{+6}$	$9.8e^{+5}$
Cumulative gas production in MSCF	$3.1e^{+5}$	$1.02e^{+6}$	$8e^{+5}$
Cumulative water production in res. bbl	3,920	64,290	$1.13e^{+5}$

Table 10 oil, gas, and water cumulative production for representative models

Water saturation maps

Matrix and fracture water saturation maps are provided in this work for each of the three models with different water saturation. All maps are captured in layer 5 which is the productive layer.

Maps were captured in the last time step.

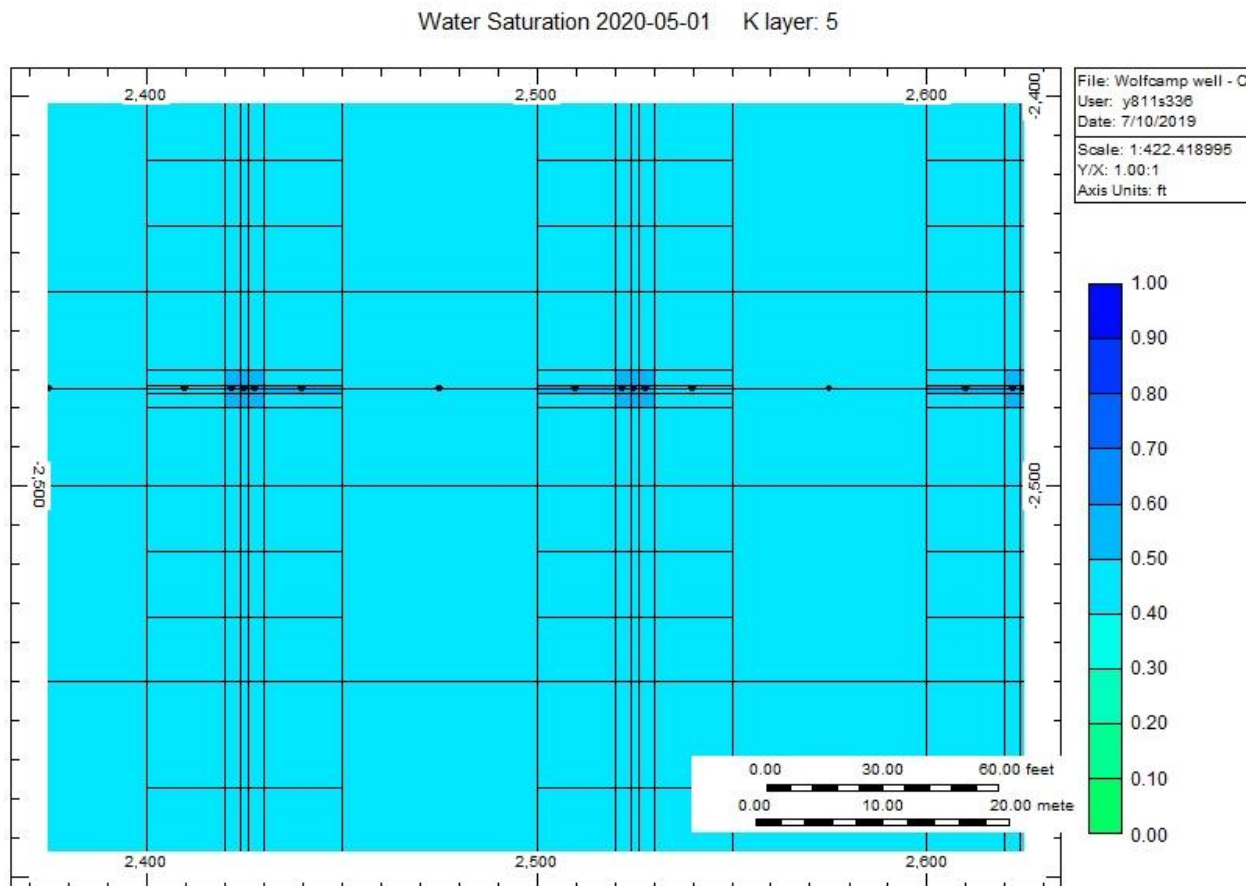


Figure 30 matrix water saturation map for the last time step for the first model with no capillary pressure

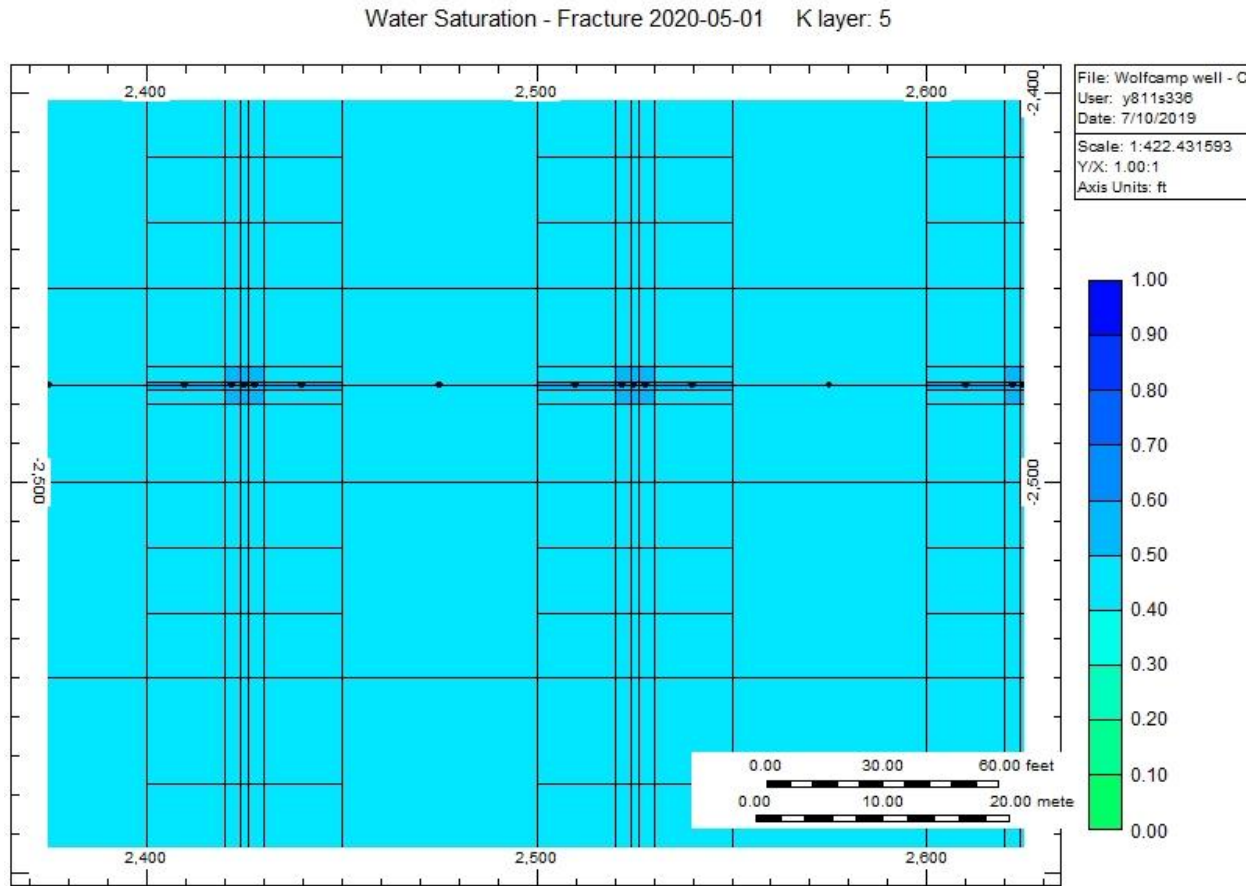


Figure 31 fracture water saturation map for the last time step for the first model with no capillary pressure

In the first model, the formation is more saturated with water near production zone. Matrix water saturation in this model is 45%, however, it increases near production zone.

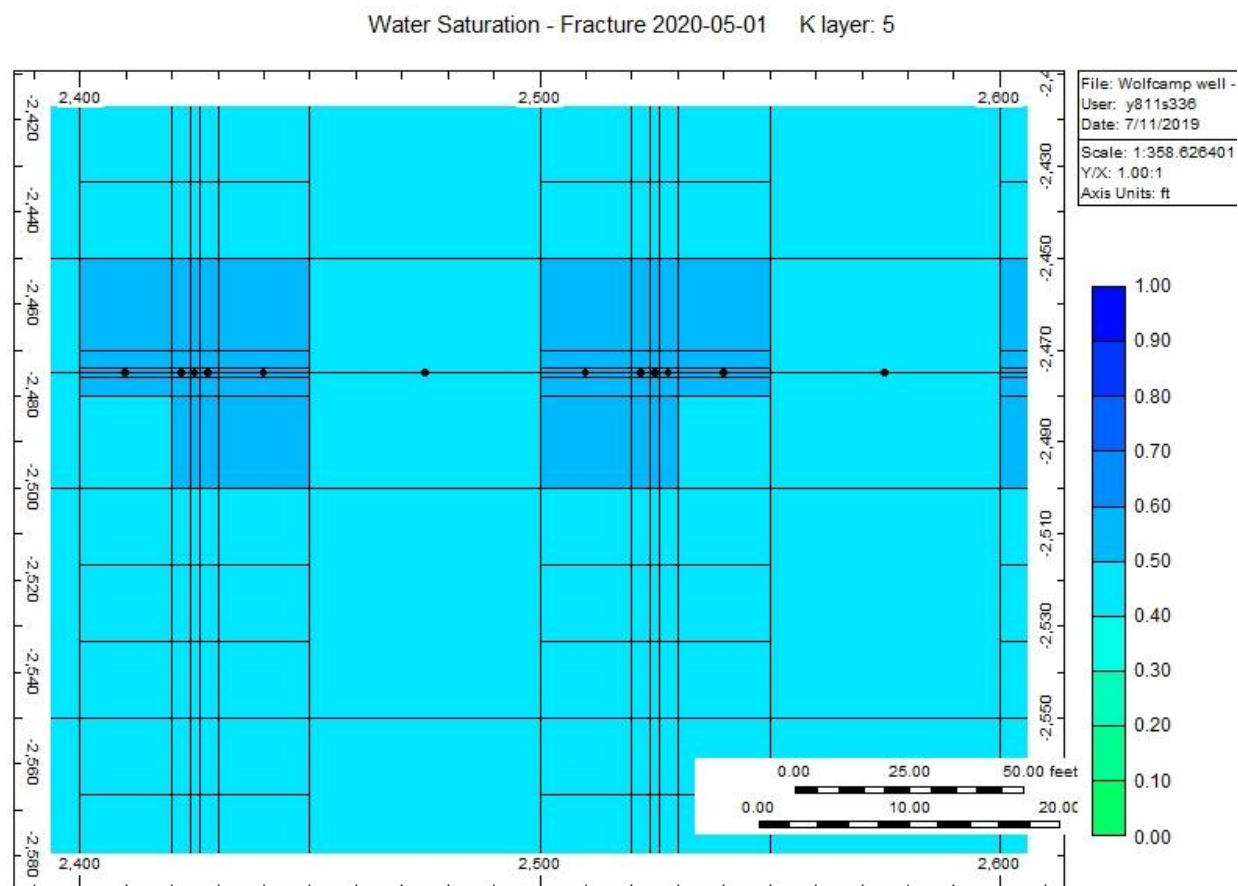


Figure 32 matrix water saturation map for the last time step for the second model with no capillary pressure

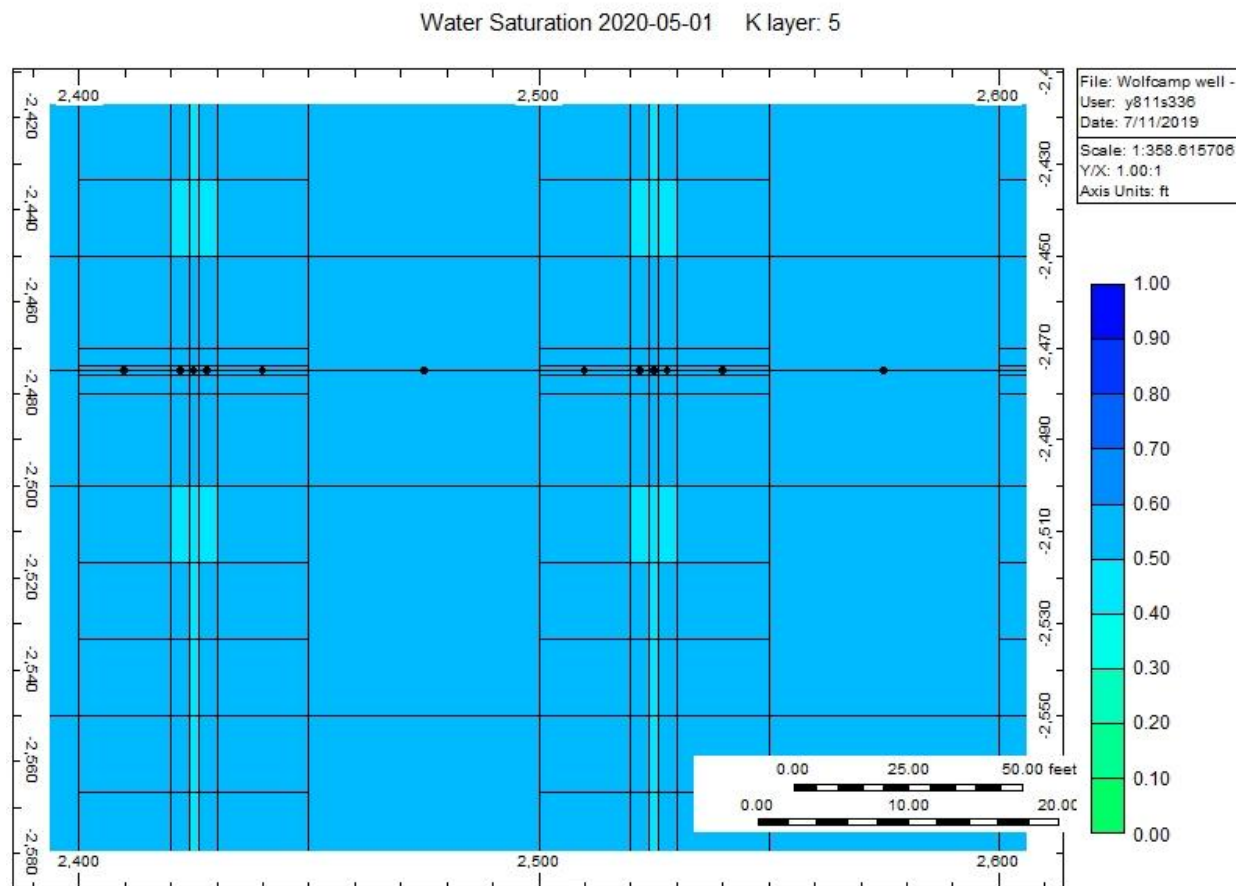


Figure 33 fracture water saturation map for the last time step for the second model with no capillary pressure

The second model has a higher water saturation and the formation is getting more saturated with water even further outside the production zone.

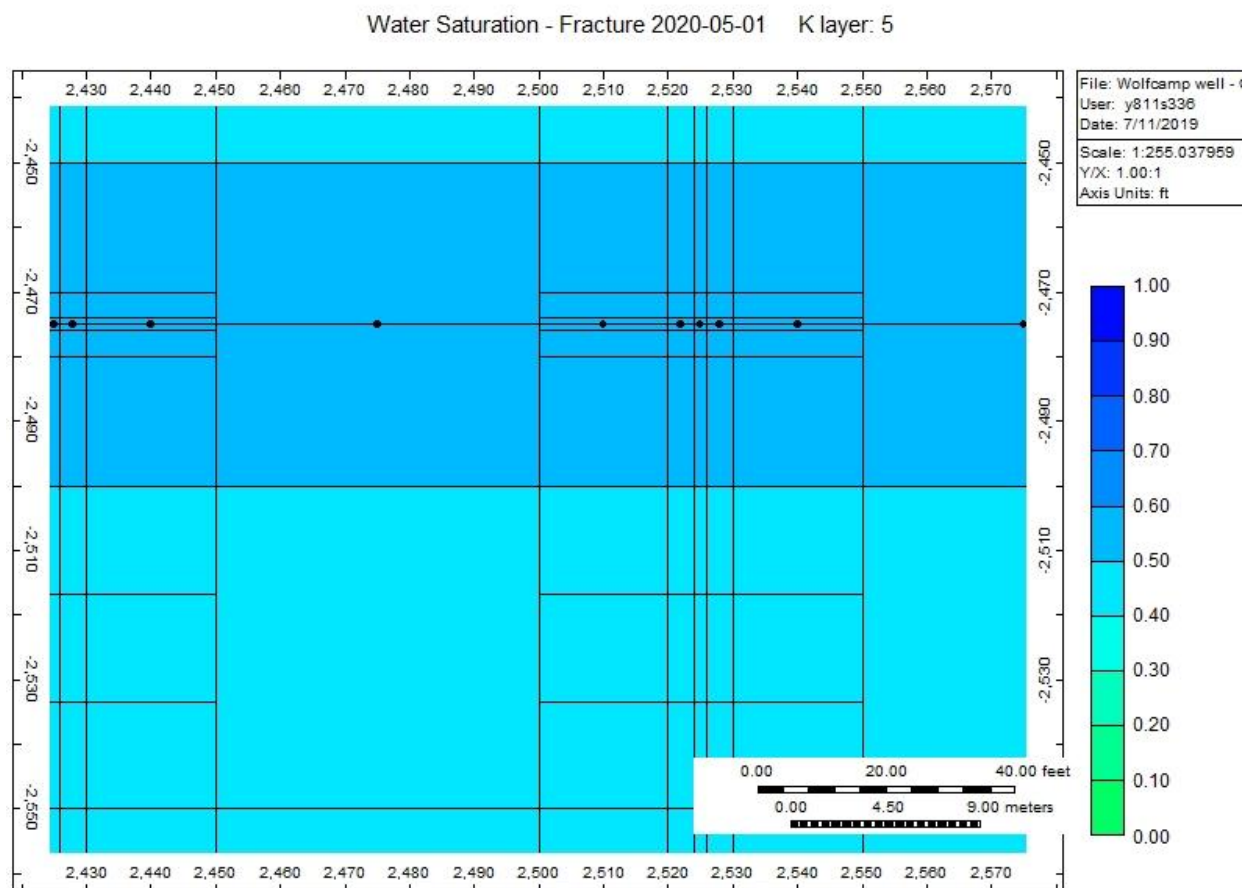


Figure 34 matrix water saturation map for the last time step for the third model with no capillary pressure

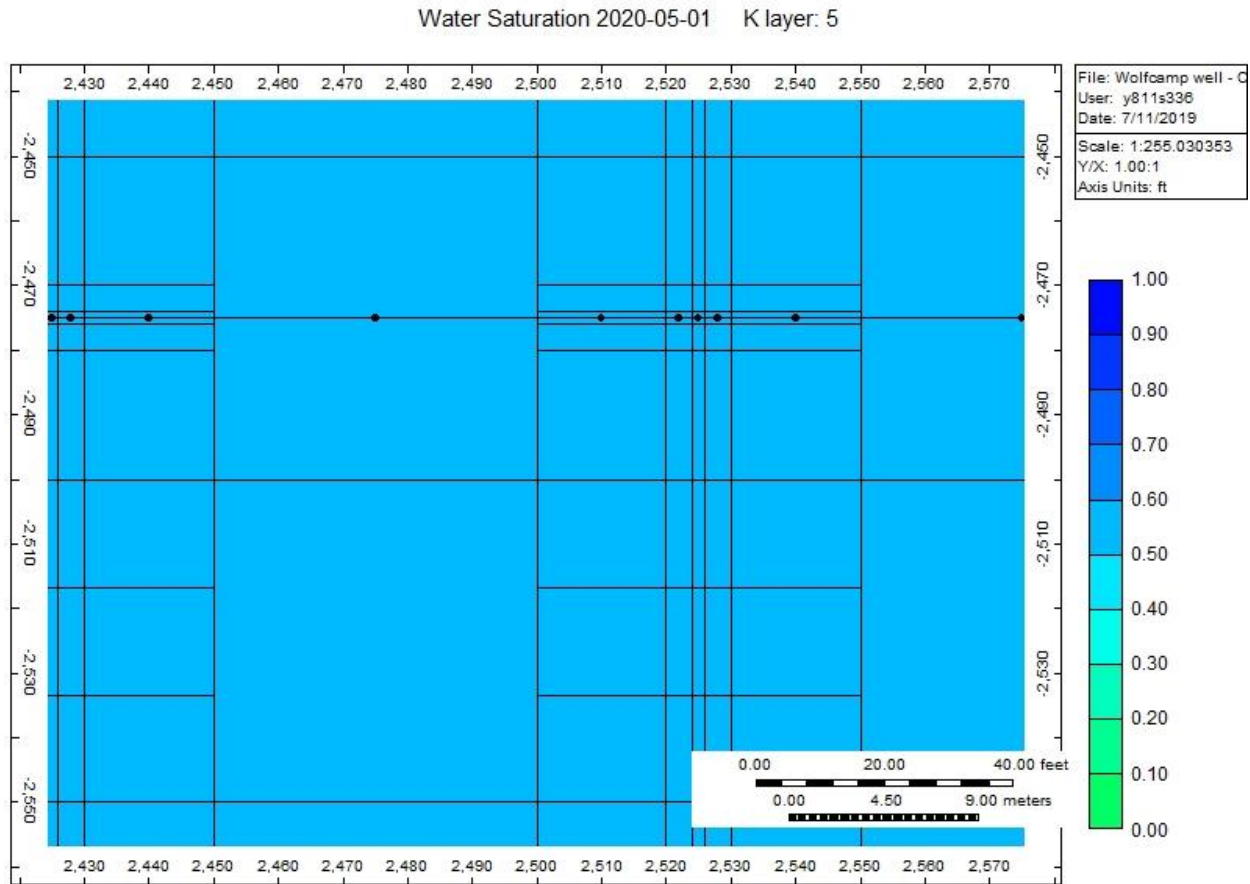


Figure 35 fracture water saturation map for the last time step for the third model with no capillary pressure

The last model had the highest water saturation. As we can see the formation near the reservoir is getting more and more saturated with water.

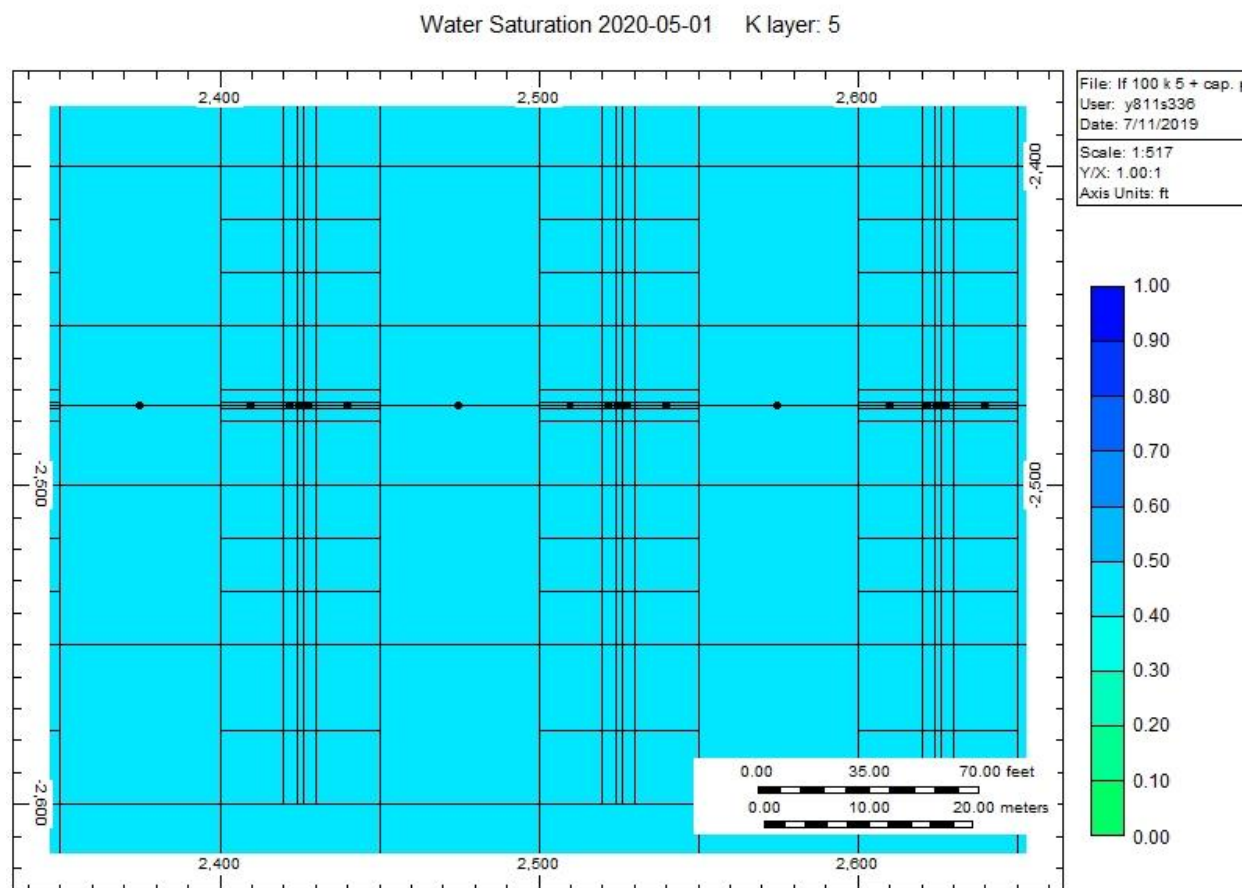


Figure 36 matrix water saturation map for the last time step for the first model with capillary pressure

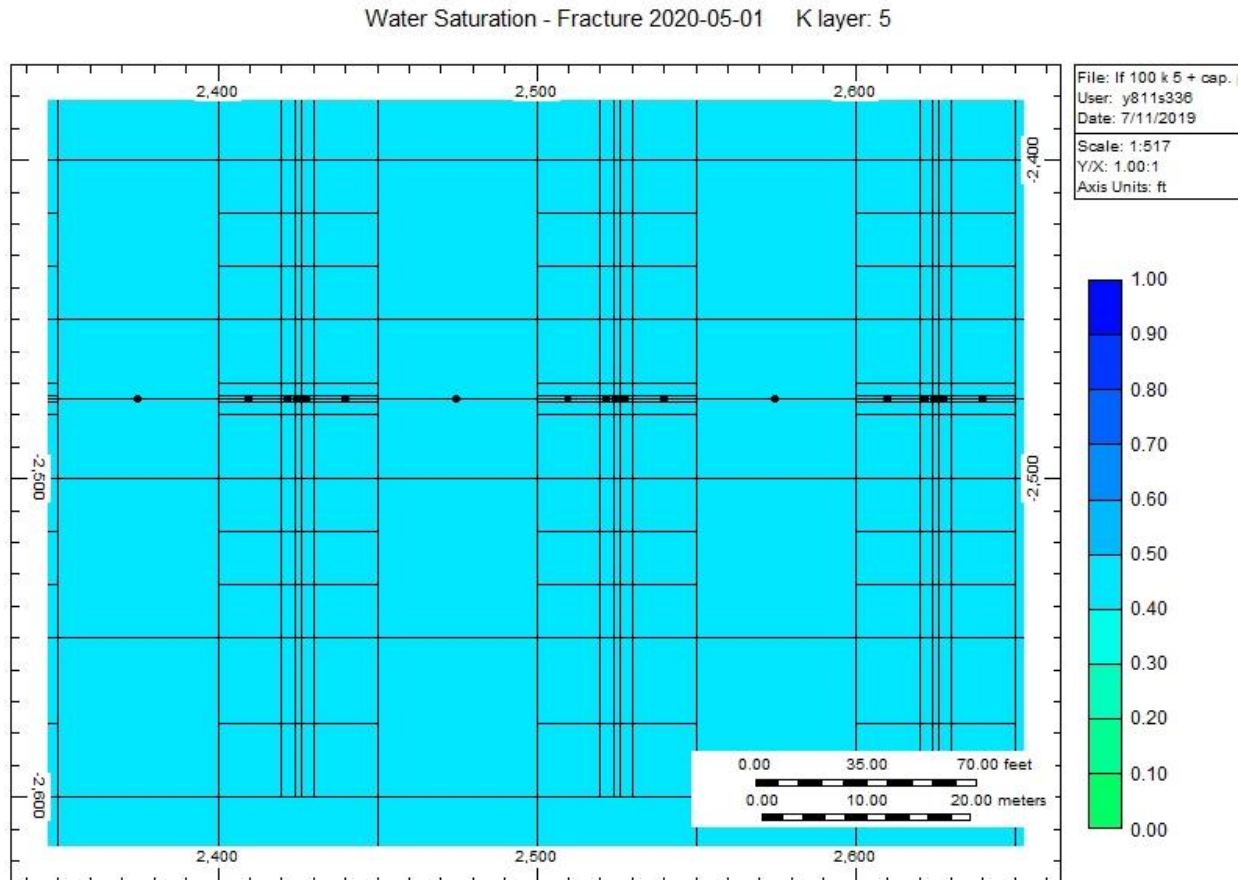


Figure 37 fracture water saturation map for the last time step for the first model with capillary pressure

Capillary pressure was added to the three models and water saturation was the same.

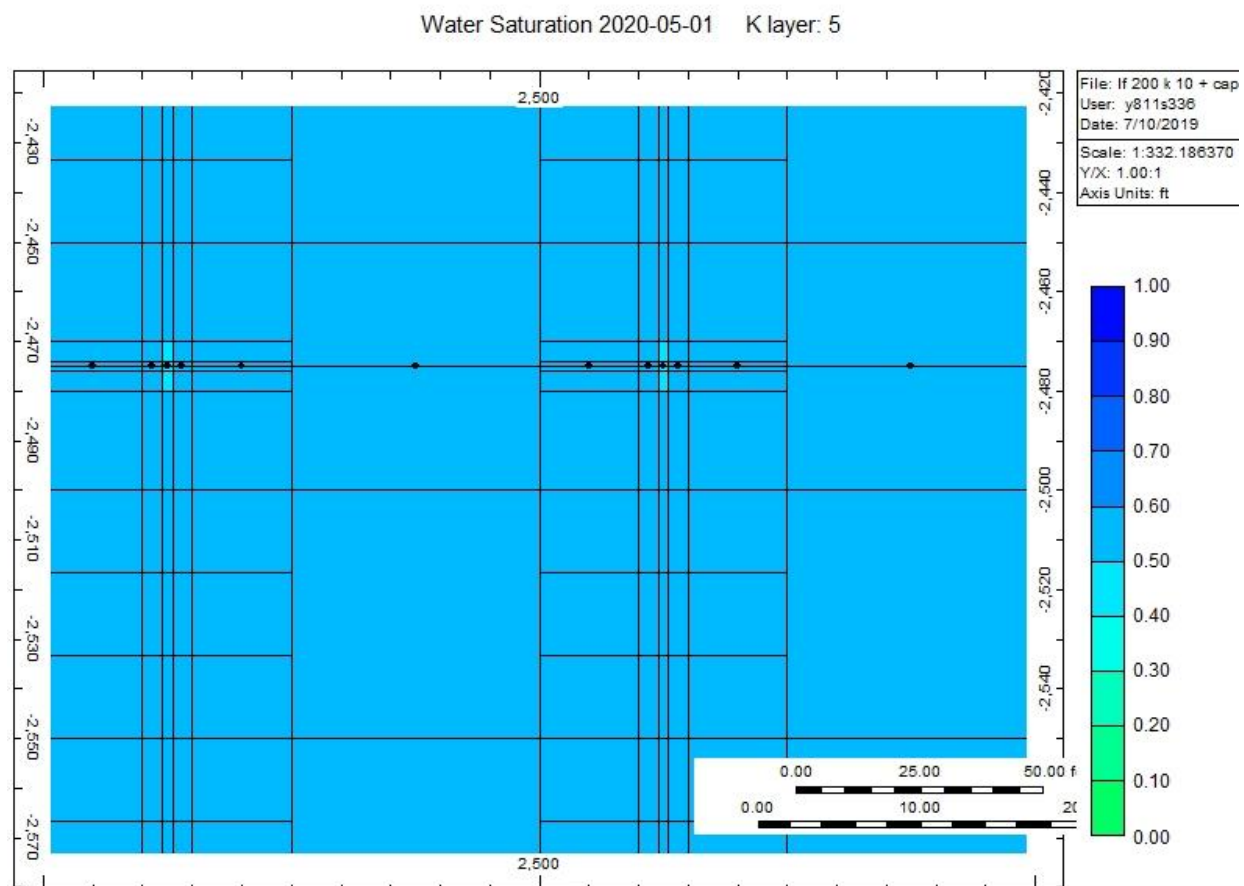


Figure 38 matrix water saturation map for the last time step for the second model with capillary pressure

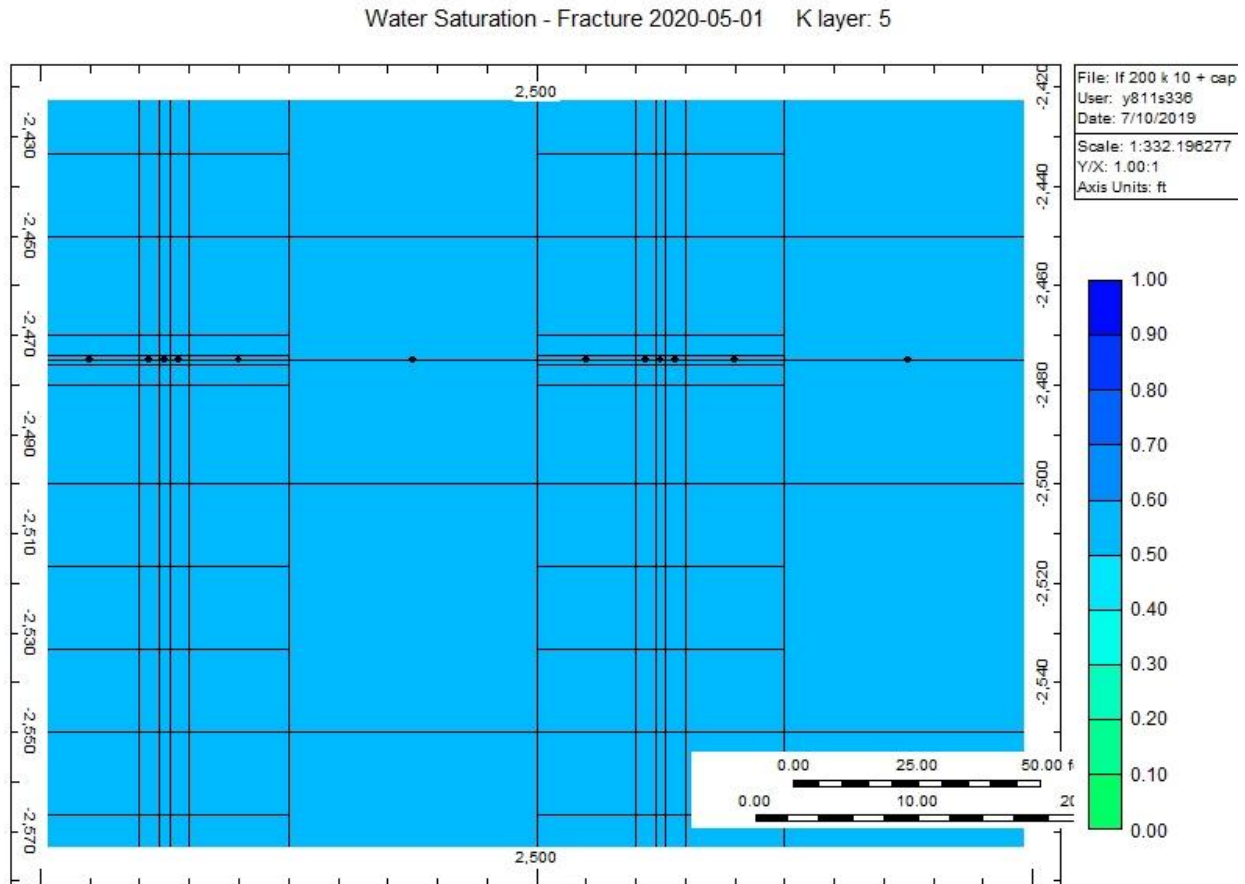


Figure 39 fracture water saturation map for the last time step for the second model with capillary pressure

As we added capillary pressure the formation got more and more saturated with water near the reservoir.

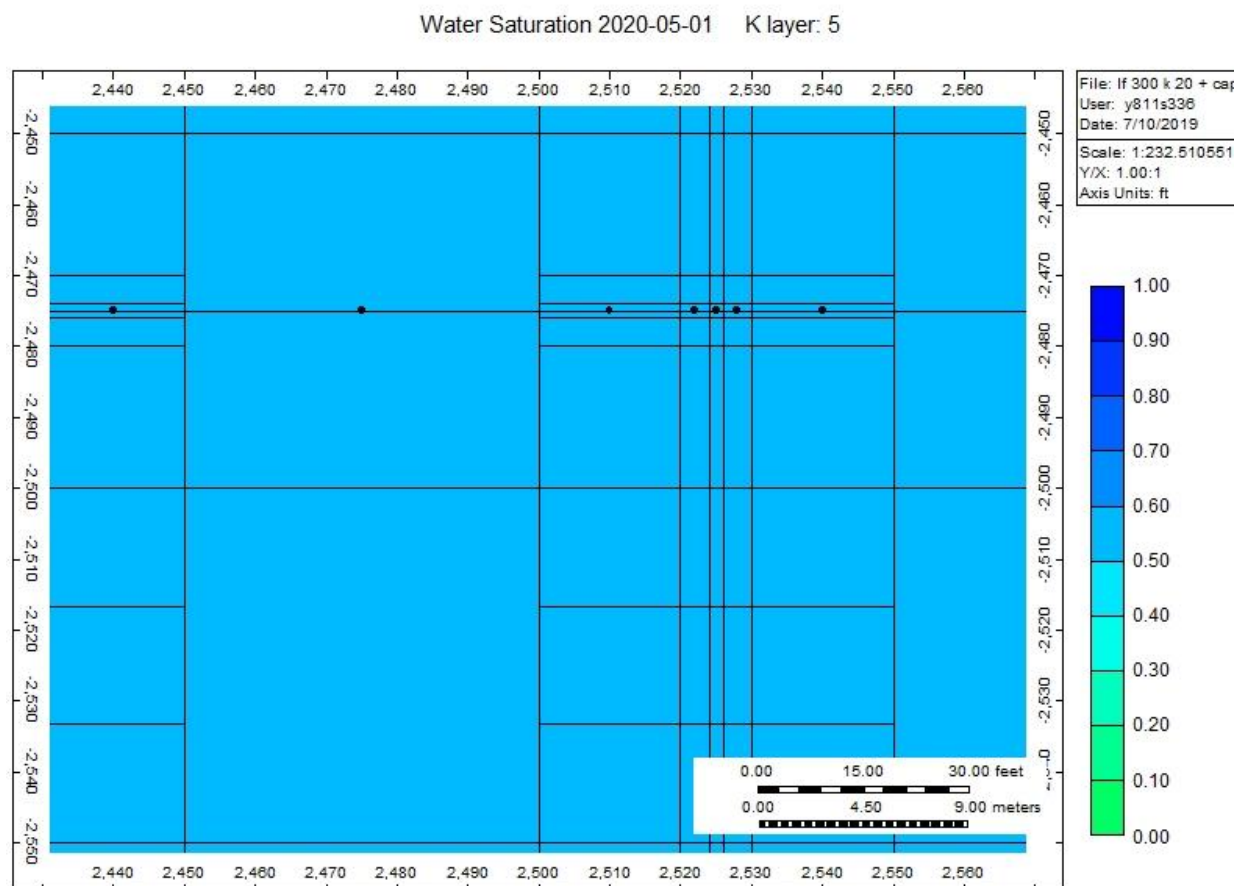


Figure 40 matrix water saturation map for the last time step for the third model with capillary pressure

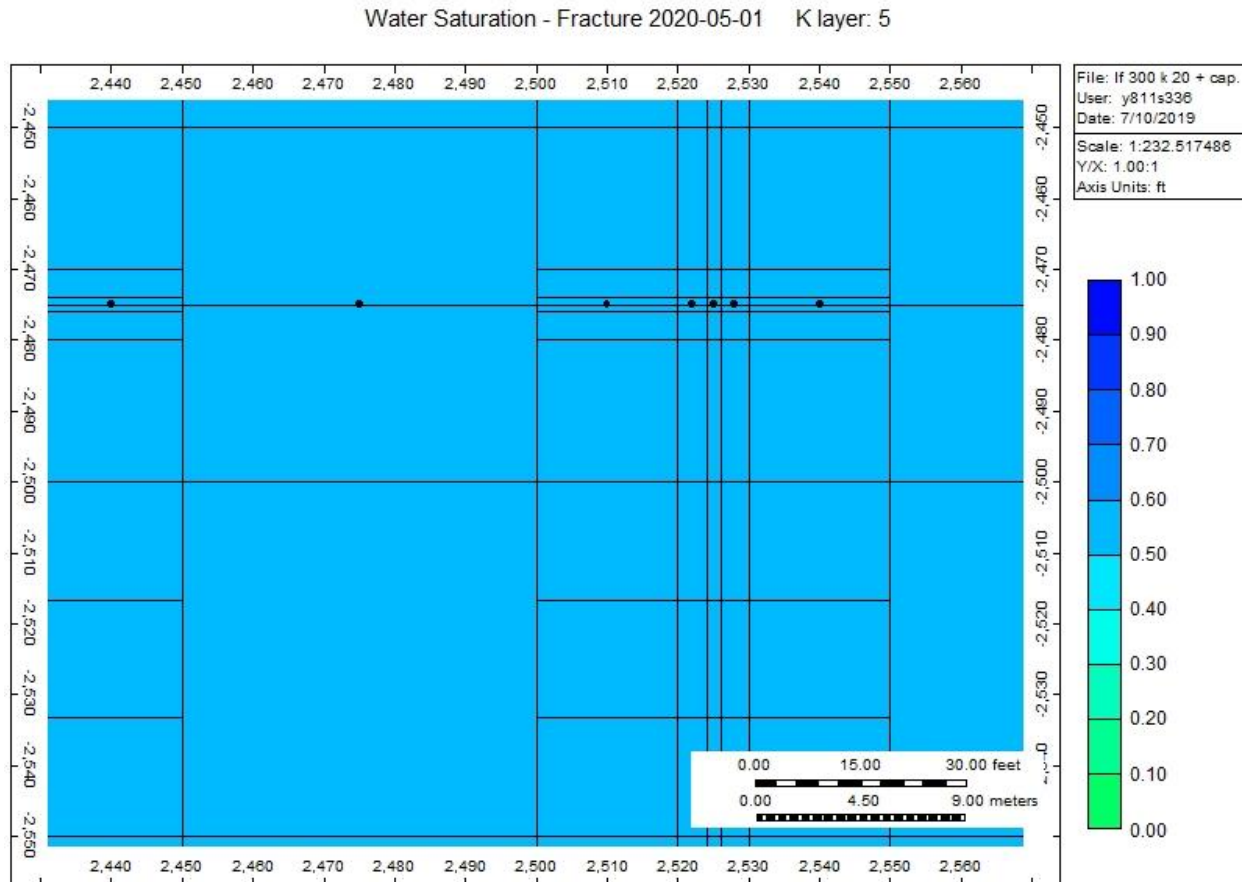


Figure 41 fracture water saturation map for the last time step for the third model with capillary pressure

Matrix and fracture maps showed that a larger area of the formation was saturated with water as capillary pressure was added.

Optimum fracture half-length

Previous results showed that the model with $X_f = 200$ ft had the highest hydrocarbon production.

We wanted to locate the peak of hydrocarbon production in Wolfcamp formation by changing fracture half-length. So we created a model with $X_f = 250$ ft, $k = 10$ md, and $S_w = 51.5\%$.

hydrocarbon production graph is shown in figure 41.

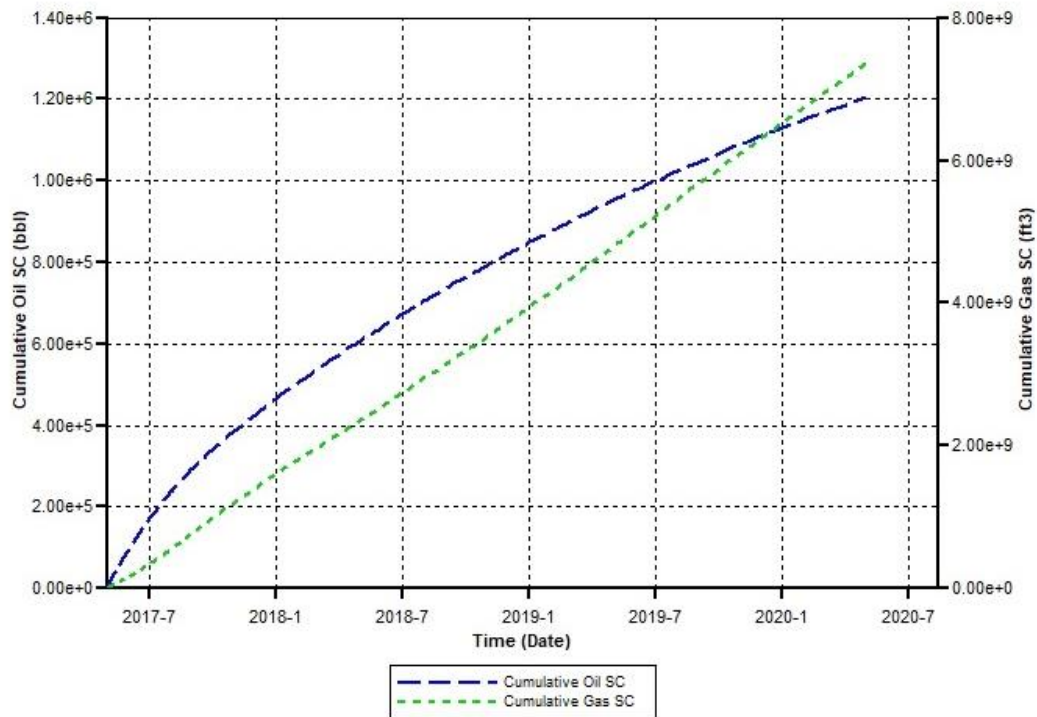


Figure 42 Oil and gas production for model with $X_f = 250\text{ft}$, $k = 10\text{md}$, and $S_w = 51.5\%$

Oil production is lower than the model with $X_f = 200\text{ft}$, however, gas production is much higher than the same model. Yet, we're interested in oil production because of lack of demand in gas production nowadays in the Permian basin.

Effect of Capillary pressure

Capillary pressure was added to all models. It ranged from 0 up to 100 psi. Each model had the exact same pressure distribution yet different permeability, water saturation, and fracture half-length. Because of the capillary pressure, water production decreased significantly while oil and gas production increased slightly. The trend was the same though, the third model had the highest water production. This model's oil, gas, and water production graph will be attached below.

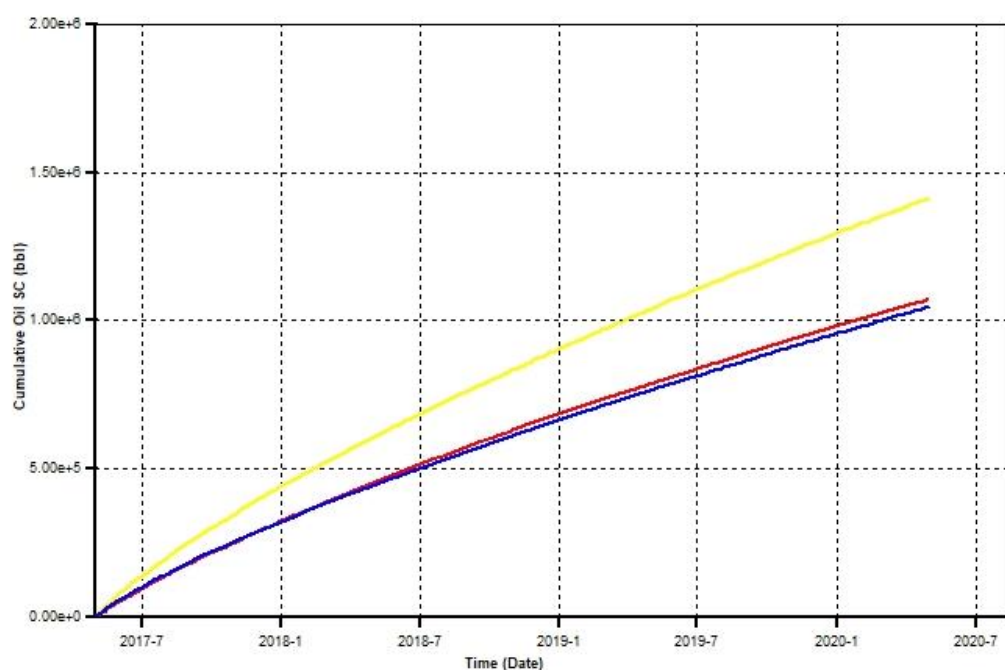


Figure 43 Cumulative oil production for the 3 representative models with capillary pressure

$X_f = 100\text{ft}$, $k = 5\text{md}$, $S_w = 45\%$

$X_f = 200\text{ft}$, $k = 10\text{md}$, $S_w = 50\%$

$X_f = 350\text{ft}$, $k = 20\text{md}$, $S_w = 55\%$

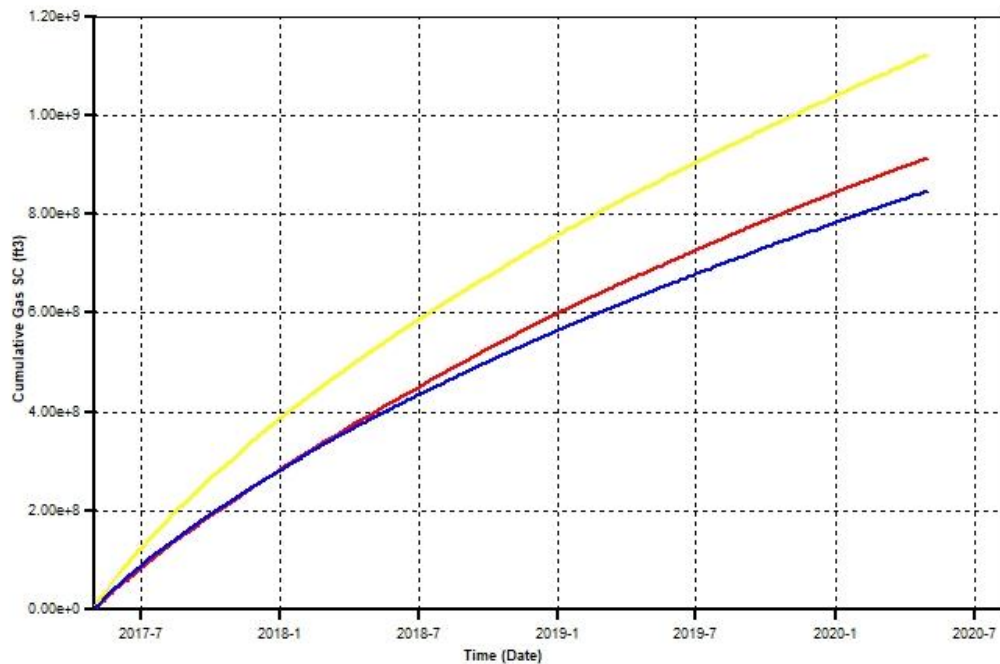


Figure 44 Cumulative gas production for the 3 representative models with capillary pressure

$X_f = 100\text{ft}$, $k = 5\text{md}$, $S_w = 45\%$

$X_f = 200\text{ft}$, $k = 10\text{md}$, $S_w = 50\%$

$X_f = 350\text{ft}$, $k = 20\text{md}$, $S_w = 55\%$

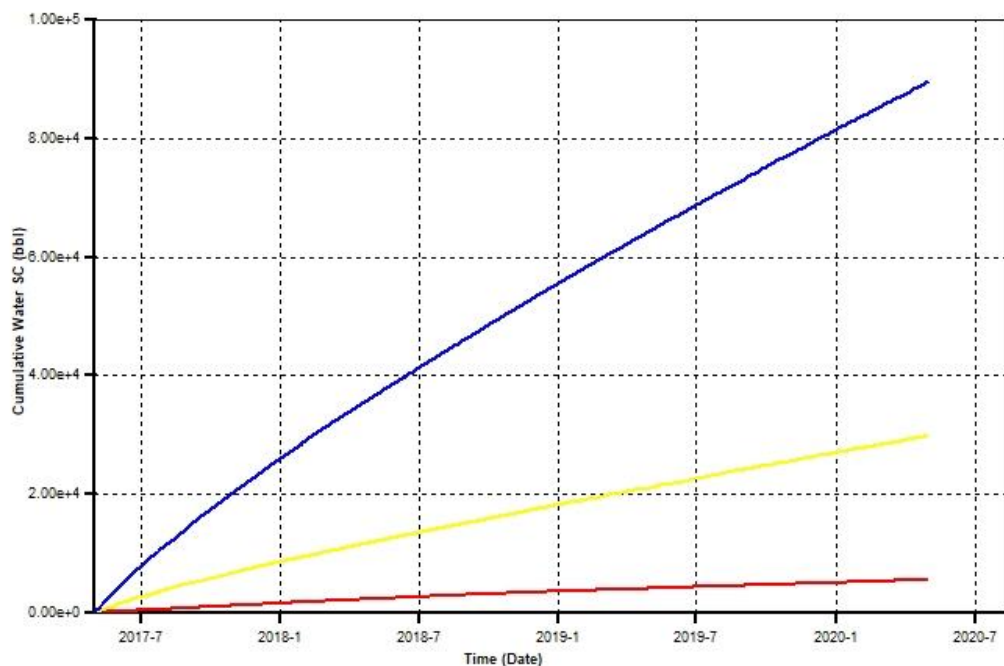


Figure 45 Cumulative water production for the 3 representative models with capillary pressure

$X_f = 100\text{ft}$, $k = 5\text{md}$, $S_w = 45\%$

$X_f = 200\text{ft}$, $k = 10\text{md}$, $S_w = 50\%$

$X_f = 350\text{ft}$, $k = 20\text{md}$, $S_w = 55\%$

In this case the 3 models' oil and gas production increased significantly for the first model and slightly for the second and third model, which was found unusual. The first model oil and gas production almost tripled compared to the same model without capillary pressure while the last two models had a decimal increase. The only explanation to the unusual increase is that since the rock is water wet, the formation imbibe water that will displace oil and gas. This process will result in higher oil and gas production. Table 4 compares oil and gas production between the three representative models with and without capillary pressure.

Table 11 Comparison between 3 representative models with and without capillary pressure

Model	Oil production, in res. bbl	Gas production in MCF
Xf = 100ft, kf = 5md, Sw = 45%, No Capillary pressure	$3.6e^{+5}$	$3.1e^{+5}$
Xf = 200ft, kf = 10md, Sw = 50%, No Capillary pressure	$1.26e^{+6}$	$1.02e^{+6}$
Xf = 350ft, kf = 20md, Sw = 55%, No Capillary pressure	$9.8e^{+5}$	$8e^{+5}$
Xf = 100ft, kf = 5md, Sw = 45% + Capillary pressure	$1.1e^{+6}$	$9.2e^{+5}$
Xf = 200ft, kf = 10md, Sw = 50% + Capillary pressure	$1.4e^{+6}$	$1.3e^{+6}$
Xf = 350ft, kf = 20md, Sw = 55% + Capillary pressure	$1.08e^{+6}$	$8.3e^{+5}$

3D water saturation map was made for the fracture and matrix for the stimulated reservoir volume (SRV) region. The maps show different saturations for different layers with different time steps along with the location of the well. Typically, the layers with the highest water saturation was the lower ones. That is due to the higher accumulation of water resulted from gravity. That was the case in the 3 models and their maps will be shown for the last time step in the productive layer in the figures section.

Economic analysis

The first model had the lowest oil and water production; therefore, it had the lowest cost of expenses. All three models cost around 7.8 million dollars for drilling and completion. Water cost for the first model was around \$300K for injection/disposal as well as oil lifting cost. The revenue from this well is 10.6 million dollars from oil and gas production and after paying all the expenses for drilling and completion.

The second model had the highest oil production and reasonable water volume so it costed a little more than the first model. Water and oil lift cost for the second model was around a million dollars. The revenue however, is more than 6 times this number after paying drilling and completion expenses. The revenues for the second model were 57 million dollars.

The last model had a little less oil production so that will lower oil lifting cost, but also had the highest water production. The cost to inject/dispose water as well as oil lifting was around a million dollars. Oil and gas revenue after paying all the drilling and completion expenses is 42.5 million dollars. A summarized table will be attached below with all the numbers to demonstrate further the analysis.

First model analysis. $X_f = 100\text{ft}$

Table 12 First model economic analysis

Expenses	Inj. Water volume	Produced water volume	Total water cost	Oil lift	Gas production	Gas lift
Amount	6500 bbl	3900bbl	\$ 8,200	360000 bbl	310000000 ft	310000000 ft

Cash flow	- \$ 2,300	- \$ 8,200		- \$ 270,000	\$ 11,000,000	\$230,000
--------------	------------------	------------------	--	-----------------	------------------	-----------

Second model analysis. $X_f = 200ft$

Table 13 Second model economic analysis

Expenses	Inj. Water volume	Produced water volume	Total water cost	Oil lift	Gas production	Gas lift
Amount	110,000bbl	64,000 bbl	\$ 130,000	1,300,000 bbl	1,000,000,000 ft	1,000,000,000 ft
Cash flow	- \$ 38,000	- \$ 96,000		\$ 940,000	\$ 57,000,000	\$750,000

Third Model analysis. $X_f = 350ft$

Table 14 Third model economic analysis

Expenses	Inj. Water volume	Produced water volume	Total water cost	Oil lift	Gas production	Gas lift
Amount	190,000 bbl	110,000 bbl	\$ 240,000	980,000 bbl	800,000,000 ft	800,000,000 ft
Cash flow	- \$ 66,000	- \$ 170,000		\$ 730,000	\$ 42,000,000	\$600,000

--	--	--	--	--	--	--

After calculating a month by month cash flow, PV was calculated for each year. At the beginning, which is considered to be year 0, the PV was the amount paid or the expenses. A summarized table of the PV for the 3 models will be attached below.

Table 15 PV table

	Model 1	Model 2	Model 3
Year 0	\$ -8,000,000	\$ -8,900,000	\$ - 8,800,000
Year 1	\$ -618100.5032	\$ 16,251,675.3	\$ 11,000,000
Year 2	\$ 4,000,000	\$ 29,000,000	\$ 21,000,000
Year 3	\$ 7,000,000	\$ 38,000,000	\$ 28,000,000

NPV was calculated after PV and it is basically the sum of each row for each model. The NPV for the first model is around \$2MM. The second model's net present value was around \$74MM which was the highest. The last model had net present value equals to \$51MM. As the NPV increases the IRR increases, therefore the IRR trend for the three models is the same as the NPV trend. Both will be summarized in the table below.

Table 16 NPV and IRR

	Model 1	Model 2	Model 3
NPV	\$ 2,300,000	\$ 74,000,000	\$ 51,000,000
IRR	9.75%	225%	161%

Based on the numbers, economically speaking, the second model is the most beneficial model among the others and the one with the highest rate of return. If a company wants to invest in one

of the three model, the IRR shows that the risk is at its lowest in the second model. This whole thing shows the importance of controlling the amount of injected water. Having a comparable simulation will always provide multiple choices and only one of them will be the most attractive. This simple process could lead to huge savings and high revenues.

Choosing the optimum fracture half-length that will control the amount of injected water will results in huge earnings. As shown previously how much difference this choice will result in. The first two models had less than 1 million dollar difference in expenses while a huge difference in revenues. This shows the importance of choosing optimum fracture half-length that will provide the well with the optimum amount of injected water.

Gas Production nowadays in Permian basin

Gas production in the Permian basin nowadays is becoming an issue for companies due to lack of demand. Companies are required to get rid of the gas they produce if it was not sold and that is costing them money. Another economic analysis was done for this scenario that brought down the revenues for hydrocarbon production. Assuming that it cost -\$0.5 to get rid of the produced gas, oil and gas revenues decreased around a million dollar for each model.

Table 17 Expenses table

	Water cost \$0.35/bbl	Water disposal cost \$1.5/bbl	Oil lift cost \$0.75/bbl	Drilling and completion cost	Gas cost	Total
Model 1	\$ 2,300	\$ 8,200	\$ 267,000	\$7.7M	\$200,000	\$8,200,000

Model 2	\$ 37,500	\$ 96,000	\$ 944,000	\$7.8M	\$500,000	\$9,400,000
Model 3	\$ 66,200	\$ 170,000	\$ 733,000	\$7.9M	\$400,000	\$9,300,000

Table 18 Revenues table

Model	Oil @ \$50/bbl	Net income
Model 1	\$18,000,000	\$10,000,000
Model 2	\$63,000,000	\$54,000,000
Model 3	\$49,000,000	\$40,000,000

Table 19 NPV and IRR for case where gas price is -\$0.5

	Model 1	Model 2	Model 3
NPV	\$ 1,566,471	\$ 72,000,000	\$ 49,000,000
IRR	6.41%	202%	146%

Cost estimate for new model

An economic analysis was made for the new model made which had the highest gas production.

This model had $X_f = 250\text{ft}$, $k = 10\text{md}$, and $S_w = 51.5\%$. Due to its high gas production, this model was not as economic as the second or even third model. As mentioned before, gas production is an extra expense nowadays in the Permian basin. Since this model had a very high gas production, gas lift price and gas dispose price are much higher in this model. Table 12 will demonstrate further.

Table 20 Expenses

	Water cost \$0.35/bbl	Water disposal cost \$1.5/bbl	Oil lift cost \$0.75/bbl	Drilling and completion cost	Gas lift cost	Total
$X_f = 250\text{ft}$, k $=10\text{md}$, $S_w =$ 51.5%	\$ 15,000	\$ 39,000	\$ 903,000	\$7.7M	\$5,400,000	\$14,300,000

Table 21 Net income if gas cost -\$0.5 in Permian basin

Xf = 250, k = 10md, Sw= 51.5%	Oil revenue = \$60,000,000	Net income = \$39,000,000
----------------------------------	----------------------------	---------------------------

Conclusions

In conclusion, it has been proven that the amount of injected water during hydraulic fracturing will surely affect oil and gas production. Decline curve analysis was made to test if increasing the amount of injected water will always increase oil & gas production. Optimistic results were shown in the Wolfcamp formation. Therefore, CMG models were created to test the idea on wells of the same length and same number of fracturing stages to understand the underlying mechanisms.

At the beginning, 3 main models were created with different fracture half-lengths (100ft, 200ft, and 350ft). Each model then was tested with different permeability (0.1, 1, 10, 100md). As the permeability kept increasing from one model to another, oil & gas production increased. Three new models were created as representative models for each fracture half-length. Permeability in the fracture was changed and water saturation was added. The first model had fracture half-length of 100ft and permeability equal to 5md. Water saturation was added to this model and was 45%. The second model had fracture half-length of 200ft and permeability equal to 10md. Water saturation for this model was 50%. The last model had fracture half-length of 350ft and permeability equal to 20md. Water saturation for this model was 55%. Results were:

- The first model had the lowest oil, gas, and water production

- The second model had the highest oil and gas production
- The third model had the highest water production

The second model had the highest oil & gas recovery because it had the optimum fracture half-length. Since the last model had the highest water saturation and water was injected the most there, it damaged the production zone. Excess water injection would also reduce relative permeability and obstruct oil and gas flow through the production zone.

Capillary pressure was added to the three models in a uniform manner. The three models had the same pressure distribution. Results were:

- The first model had the lowest water production
- The second model had the highest oil & gas production
- The third model had the lowest oil & gas production and the highest water production

Choosing the optimum fracture half-length will result in injecting the perfect amount of water.

Injecting the optimum amount of water will always result in the best hydrocarbon production. In other words, this whole process will result in the best revenues we can get from the well and the most profitable without causing any damage to the formation.

Nomenclature

X_f : fracture half-length

k : permeability

S_w : Water saturation

P_c = capillary pressure

SRV = stimulated reservoir volume

PV = Present value

NPV = Net present value

IRR = Internal rate of return

Figures

Second segment graphs:

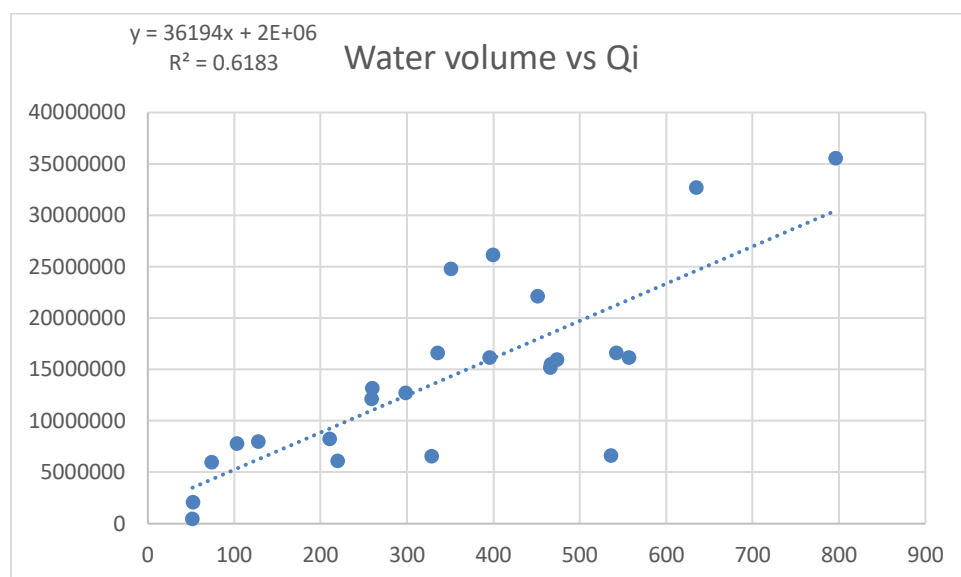


Figure 46 Injected water volume in Gallon vs Qi

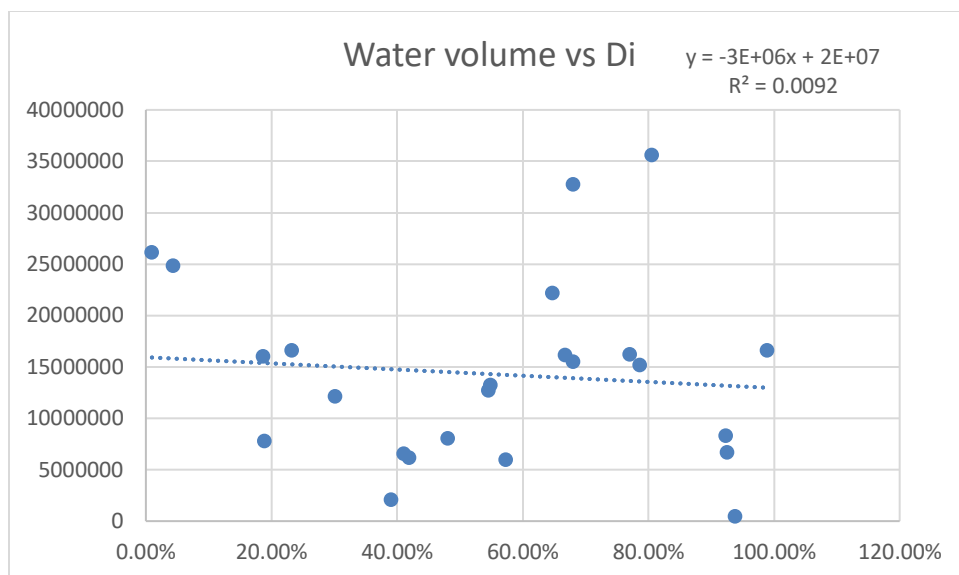


Figure 47 Injected water volume in Gallon vs Di

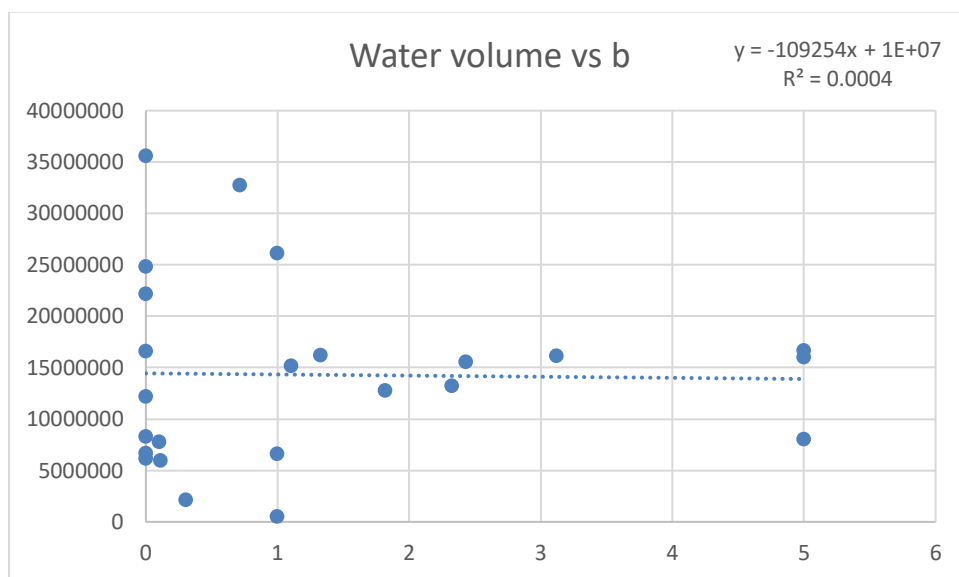


Figure 48 Injected water volume in Gallon vs b

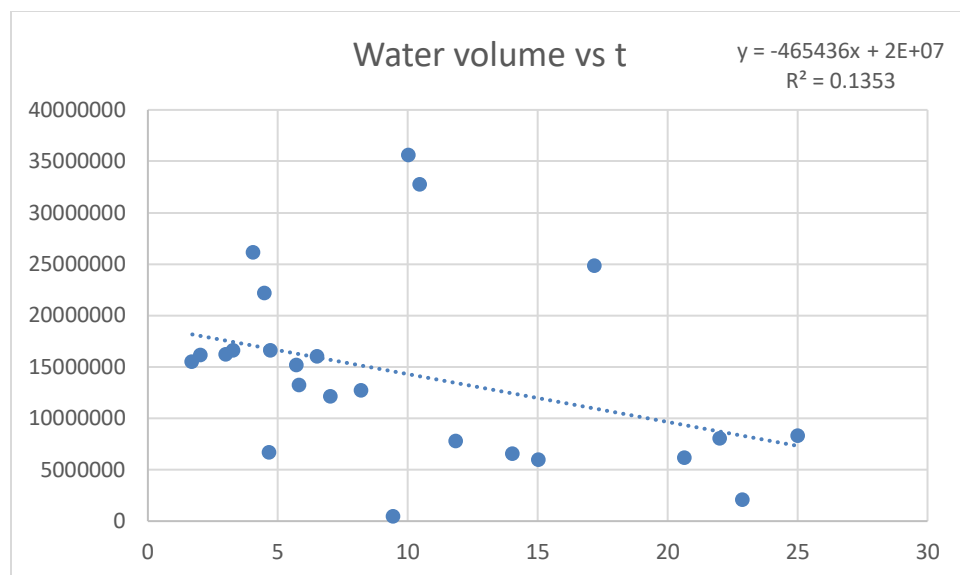


Figure 49 Injected water volume in Gallon vs time in months

Third segment graphs

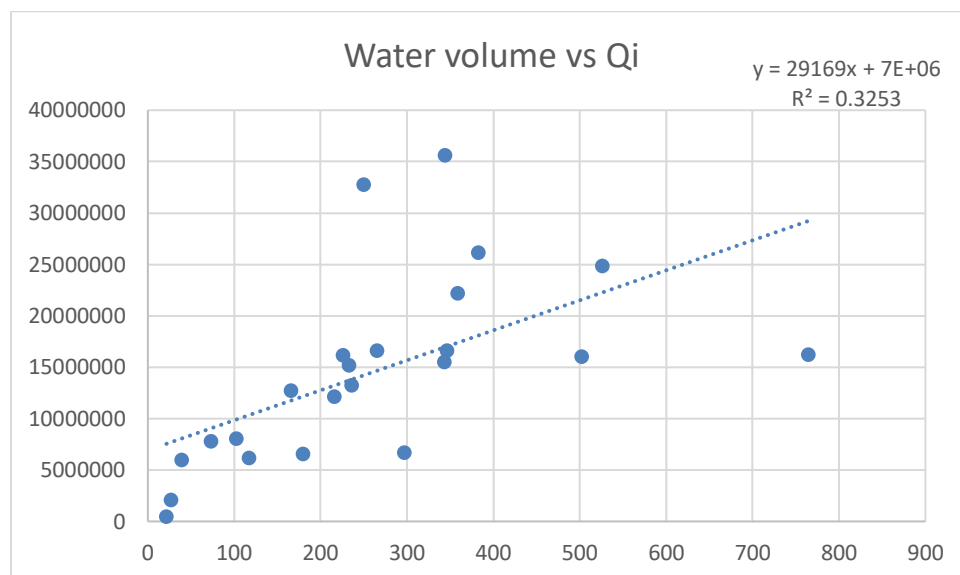


Figure 50 Injected water volume in Gallon vs Qi

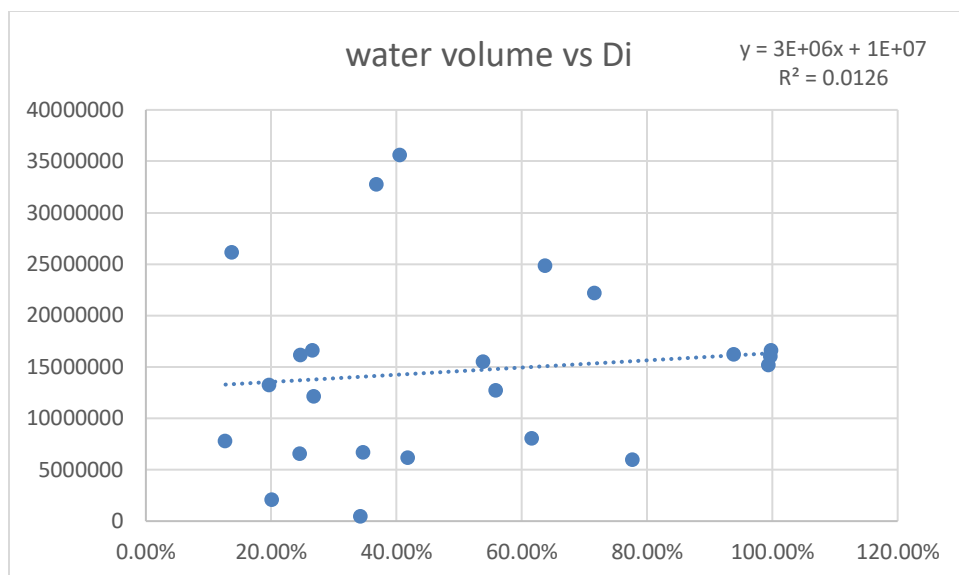


Figure 51 Injected water volume in Gallon vs Di

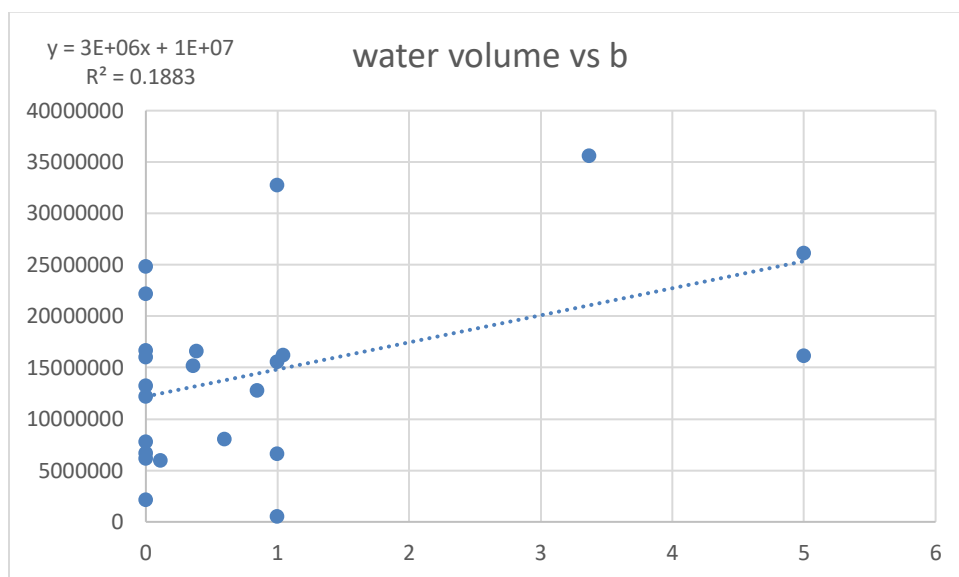


Figure 52 Injected water volume in Gallon vs b

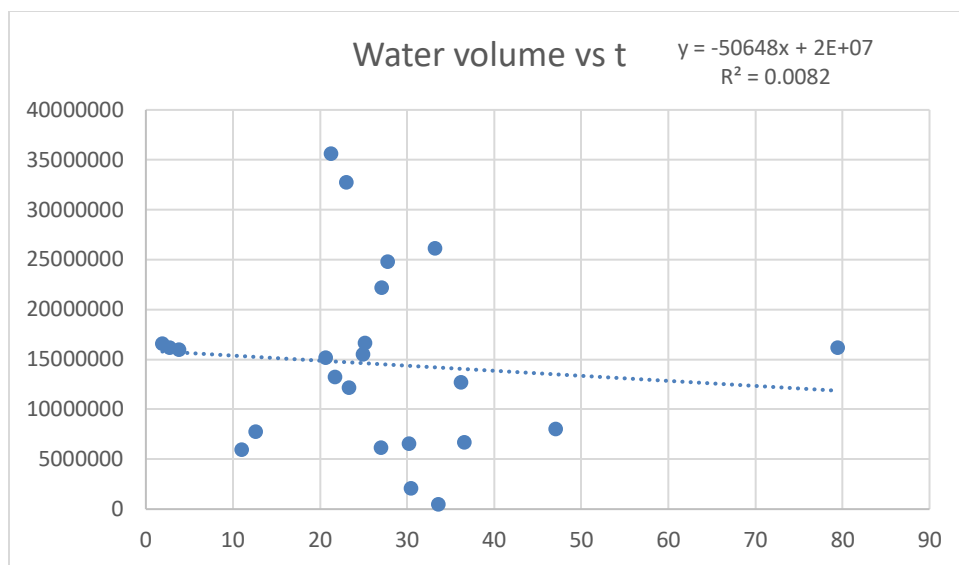


Figure 53 Injected water volume in Gallon vs time in months

4th segment graphs

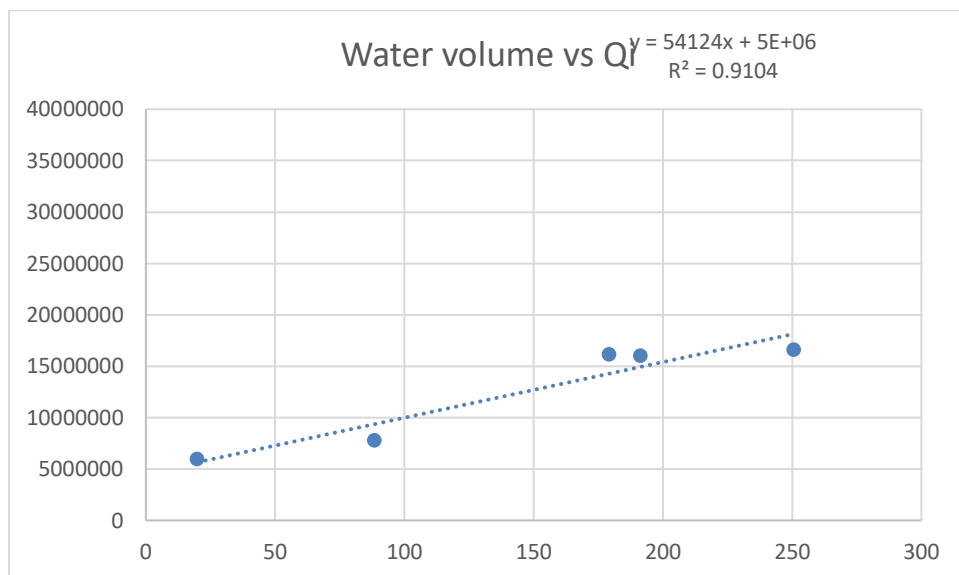


Figure 54 Injected water volume in Gallon vs Q_i

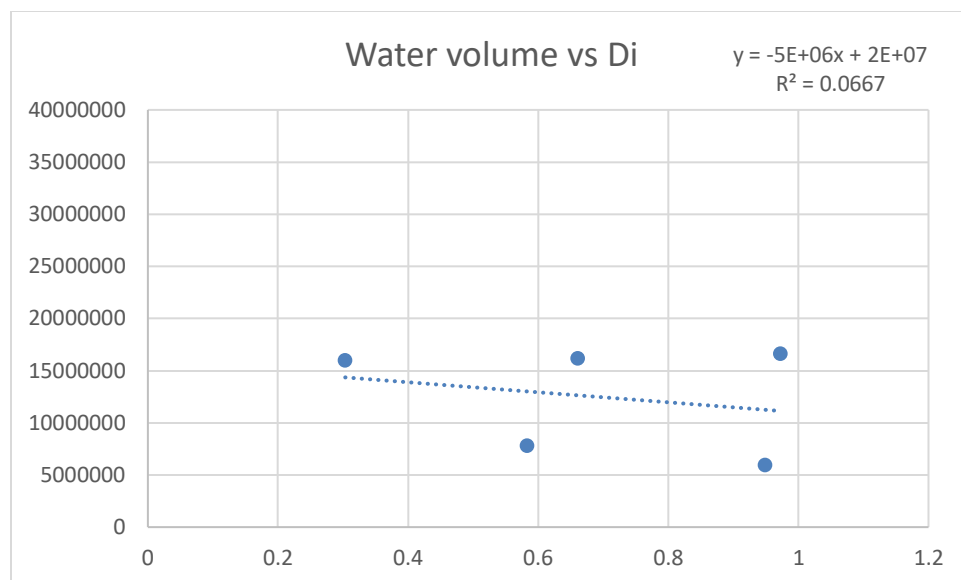


Figure 55 Injected water volume in Gallon vs Di

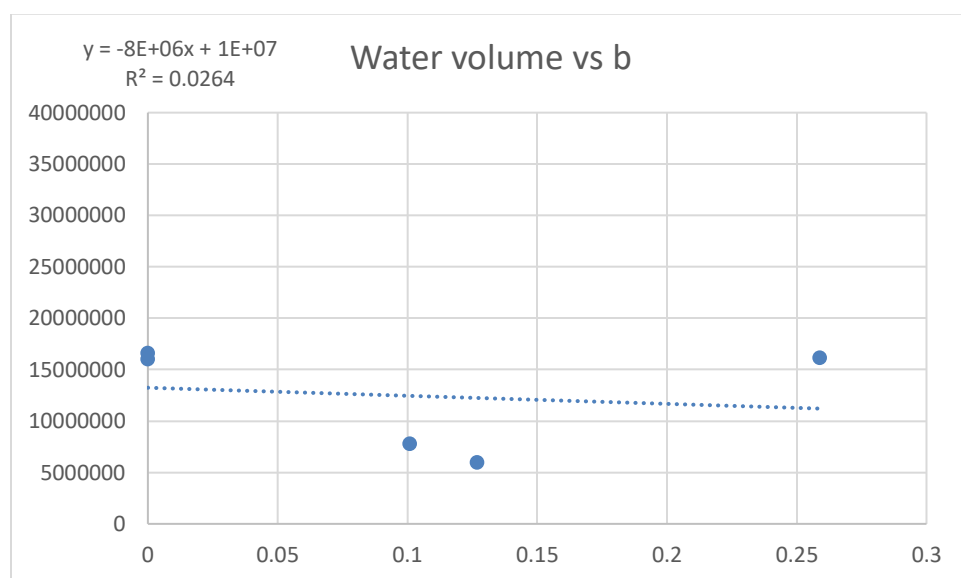


Figure 56 Injected water volume in Gallon vs b

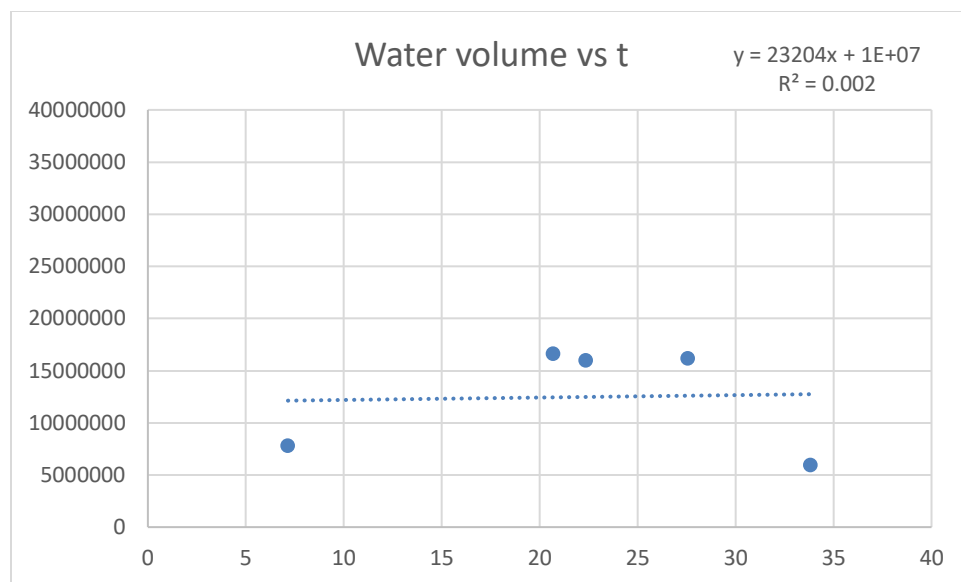


Figure 57 Injected water volume in Gallon vs time in months

5th segment graphs

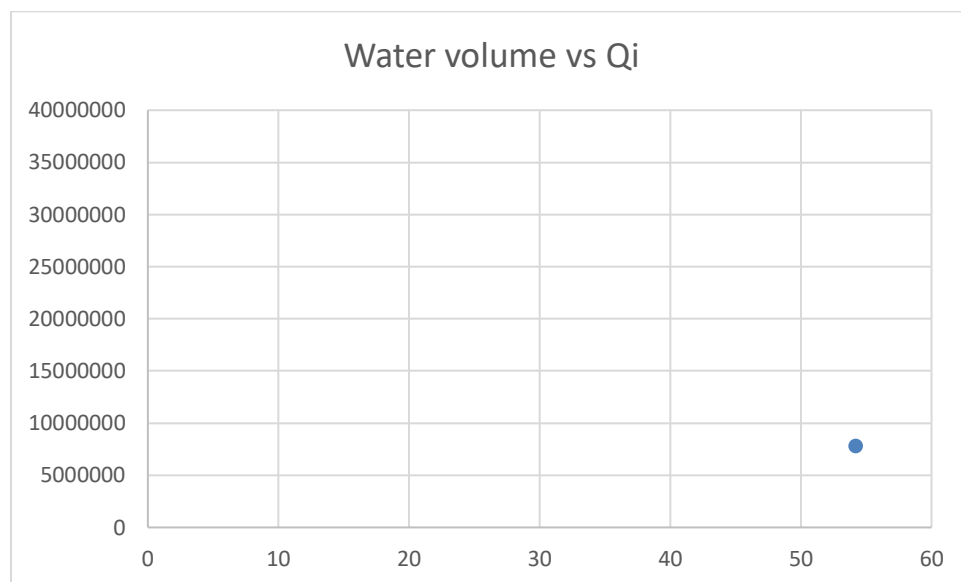


Figure 58 Injected water volume in Gallon vs Qi

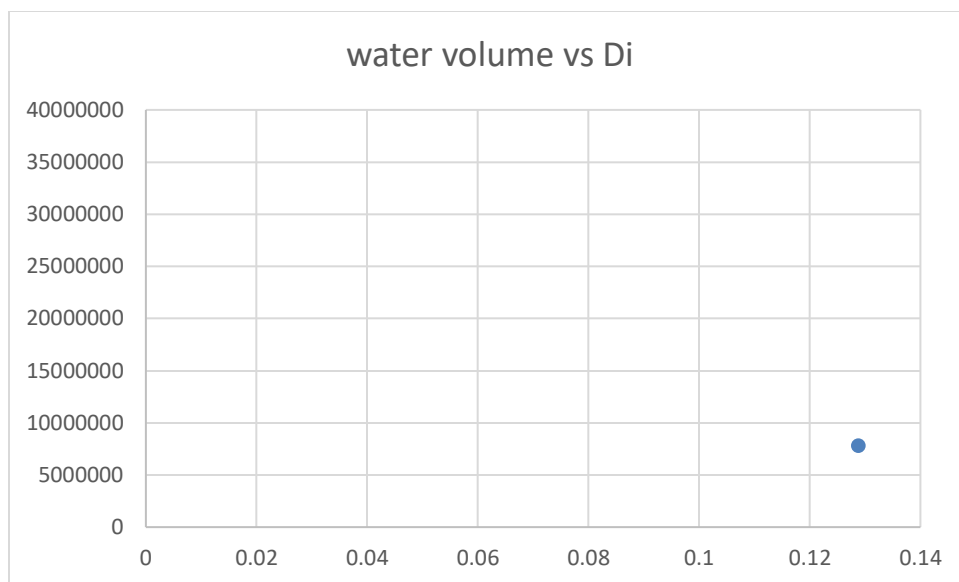


Figure 59 Injected water volume in Gallon vs Di

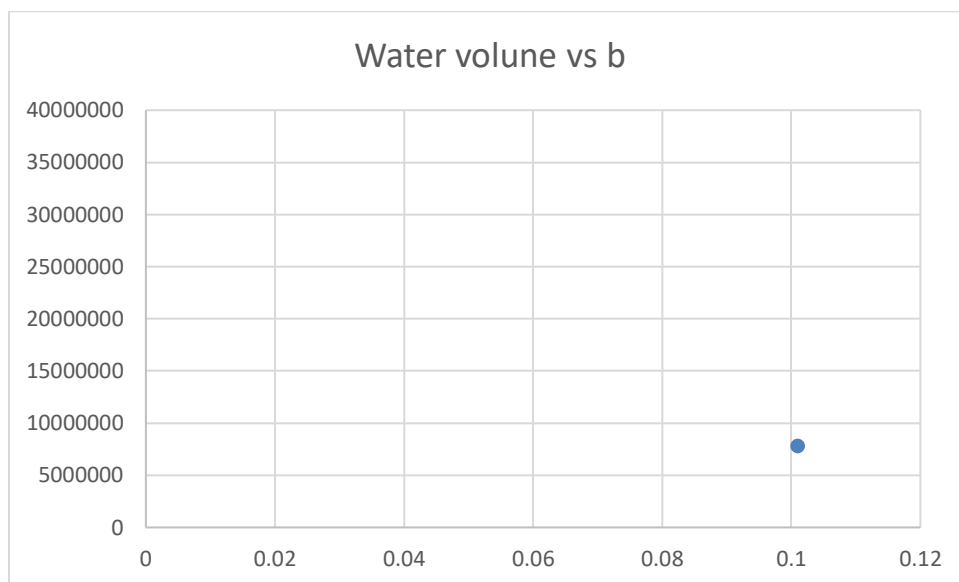


Figure 60 Injected water volume in Gallon vs b

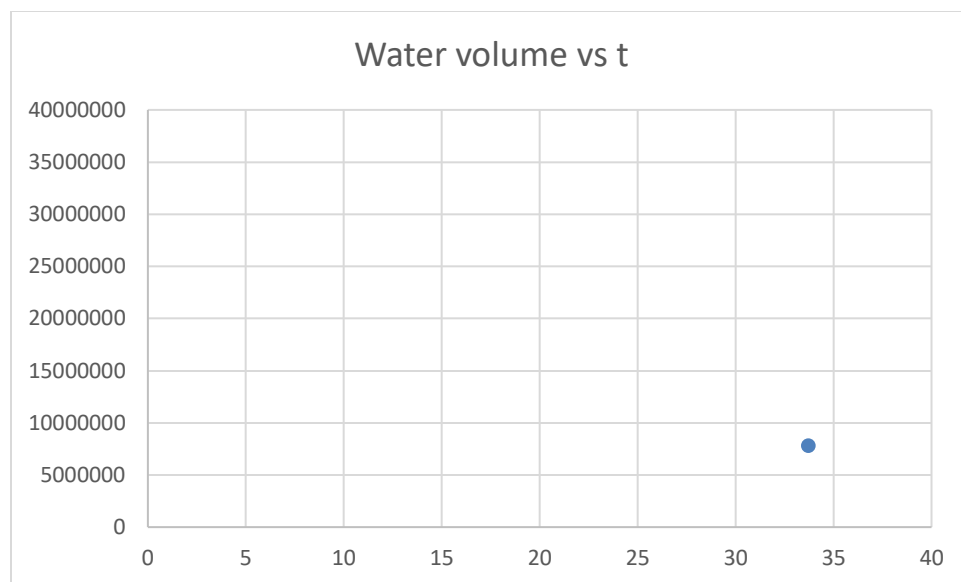


Figure 61 Injected water volume in Gallon vs time in months

References

- AAPG wiki*. (2016, February 2). Retrieved from Permeability: <https://wiki.aapg.org/Permeability>
- Arps, J. J. (1945, December). Petroleum Economics. *Analysis of Decline Curves*, 160(01), 228-247. doi:<https://doi.org/10.2118/945228-G>
- B3. (2019, 02 26). *Permian Water Outlook*. Retrieved from Groundwater Protection Council: http://www.gwpc.org/sites/default/files/event-sessions/Produced%20Water%20-%20Rob%20Bruant_0.pdf
- Barati, R., & Aghababa, H. (2016). Hydraulic Fracturing Fluids and Production. In M. R. Riazi, *Exploration and Production of Petroleum and Natural Gas* (pp. 366-369). Mayfield, PA: ASTM International.
- Barati, R., Hutchins, R., Friedel, T., Ayoub, J., Dessinges, M., & England, K. (2009). Fracture Impact of Yield Stress and Fracture-Face Damage on Production With a Three-Phase 2D Model. *SPE Production and Operation* (pp. 336-345). Lafayette, Louisiana: SPE.
- Bennion, D., Thomas, F., Schulmeister, B., & Romanova, U. (2006). Water and Oil Base Fluid Retention in Low Permeability Porous Media - an Update. *Canadian International Petroleum Conference* (pp. 1-10). Calgary, Alberta, Canada: Canadian Institute of Mining, Metallurgy & Petroleum.
- Chevron. (n.d.). *the permian basin*. Retrieved July 14, 2019, from [chevron.com](https://www.chevron.com/projects/permian): <https://www.chevron.com/projects/permian>
- Clarkson, C. (2013, January 11). Production data analysis of unconventional gas wells: Review of theory and best practices. *International Journal of Coal Geology*, pp. 101-146.
- Clarkson, C. R. (2013). Production data analysis of unconventional gas wells: Review of theory and best practices. *International Journal of Coal Geology*, 106.

- Collins, G. (2018). New Ways of Thinking About Oilfield Water in the Permian Basin. *ShaleTech 2018*. Houston, TX: Baker institute.
- Donham, J. (1991). Offshore Water Injection System: Problems and Solutions. *23rd Annual OTC* (pp. 773-782). Houston, Texas: Offshore Technology Conference.
- Forrest, J., Zhu, T., Xiong, H., & Pradhan, Y. (2018). The Effect of Initial Conditions and Fluid PVT Properties on Unconventional Oil and Gas Recoveries in the Wolfcamp Formation in the Midland Basin. *Unconventional Resources Technology Conference* (p. 9). Houston, Texas: Society of Petroleum Engineering.
- Fracfocus.org*. (2011). Retrieved July 15, 2019, from Fracfocus: <https://fracfocusdata.org/DisclosureSearch/Search.aspx>
- Gaswirth, S. B. (2017). *Assessment of Continuous Oil Resources in the the Wolfcamp Shale of the Midland Basin, Permian Basin Province, Texas, 2016*. Retrieved from USGS: <https://pubs.usgs.gov/of/2017/1013/ofr20171013.pdf>
- Gay, M. O., & Fletcher, S. (2014, May). *Strategies Assure Water Availability*. Retrieved from The American Oil & Gas Reporter: <https://www.aogr.com/web-exclusives/exclusive-story/strategies-assure-water-availability>
- Gou, X., Song, H., Wu, K., & Killough, J. (2017, December 16). Pressure characteristics and performance of multi-stage fractured horizontal well in shale gas reservoirs with coupled flow and geomechanics. *Journal of Petroleum Science and Engineering*, pp. 1-15.
- Gupta, I., Rai, C., Sondergeld, C., & Devegowd, D. (2017). Rock Typing in Wolfcamp Formation. *SPWLA 58th Annual Logging Symposium*, 2.
- Gupta, I., Rai, C., Sondergeld, C., & Devegowda, D. (2017). Rock Typing In Wolfcamp Formation. *SPWLA 58th Annual Logging Symposium*, 2.

IHS decline plus. (2019, July 5). Retrieved from IHS Harmony:

https://www.ihsenergy.ca/support/documentation_ca/Harmony/Default.htm#html_files/about_the_harmony_environment/ihs_declineplus.htm?Highlight=Arps

Nicot, J.-P., & Scanlon, B. R. (2012, March 2). Water Use for Shale-Gas Production in Texas, U.S. *Environmental Science & Technology*, p. 3580.

Ojha, S. P., Misra, S., Sinha, A., Dang, S., Tinni, A., Sondergeld, C., & Rai, C. (2018). Relative Permeability and Production-Performance Estimations for Bakken, Wolfcamp, Eagle Ford, and Woodford Shale Formation. *SPE Reservoir Evaluating & Engineering*, 313.

Pioneer Natural Resources Company. (2014, January 6). Retrieved from Securities and Exchange Commission: <http://investors.pxd.com/static-files/2dae9e6b-3d1f-4282-a822-a502f55e207a>

Popova, O. (2018, November). *Permian Basin*. Retrieved from U.S. Energy information Administration: https://www.eia.gov/maps/pdf/Wolfcamp_EIA_Report_Nov2018.pdf

Railroad Commission of Texas. (2014, November 3). *Hearing Division*. Retrieved from Texas Railroad Commission: <https://stage.rrc.state.tx.us/media/25456/7c-91169-1171-afr-pfd.pdf>

Railroad Commission of Texas. (2019, July 12). *Permian Basin Information*. Retrieved from Railroad Commission of Texas: <https://www.rrc.state.tx.us/oil-gas/major-oil-and-gas-formations/permian-basin-information/>

Scanlon, B. R., Reedy, R. C., Male, F., & Walsh, M. (2017). Water Issues Related to Transitioning from Conventional to Unconventional Oil Production in the Permian Basin. *Environmental Science & Technology*, 10908.

Securities and Exchange Commission. (2014, January 6). *Form 8-K*. Retrieved from investors: <http://investors.pxd.com/static-files/2dae9e6b-3d1f-4282-a822-a502f55e207a>

Stratigraphy. (n.d.). *GeoWhen database*. Retrieved July 22, 2019, from Stratigraphy:

<http://www.stratigraphy.org/bak/geowhen/stages/Wolfcampian.html>

Tayong A, R., Alhubail, M. M., Maulianda, B., & Barati, R. (2019). Simulating yield stress variation along hydraulic fracture face enhances. *Journal of Natural Gas Science and Engineering*, 39.

U.S. Energy Information Administration. (2018, October 3). *Permian Basin*. Retrieved from U.S. Energy Information Administration:

https://www.eia.gov/maps/pdf/PermianBasin_Wolfcamp_EIARReport_Oct2018.pdf

University Lands. (2019). Retrieved from University Lands:

<http://www.utlands.utsystem.edu/WellLibrary/Production>

Zhao, Y.-L., Zhang, L.-H., Luo, J.-X., & Zhang, B.-N. (2014, March 19). Performance of fractured horizontal well with stimulated reservoir volume in unconventional gas reservoir. *Journal of Hydrology*, p. 447.

Zhong, C., & Leung, J. Y. (2019). Numerical Investigation of Water Blockage in Secondary Fractures and Apparent Permeability Modeling in Shale Gas Production. *Unconventional Resources Technology Conference* (pp. 1-21). Denver, Colorado: URTeC Technical Program.

Zhu, J., Forrest, J., Xiong, H., & Pradhan, Y. (2018). Lessons Learned from Existing Horizontal Fractured Wells on University Lands in the Midland Basin: Rate Transient Analyses Vs Completion and Field Development Optimization. *Unconventional Resources Technology Conference* (p. 1). Houston, Texas: URTeC.